Electronic Supplementary Material (ESI) for Polymer Chemistry.

Supporting information

Controlling the stereoselectivity of *rac*-LA polymerization by chiral recognition induced formation of homochiral dimeric metal alkoxides

Paweł Horeglad,[a,*] Martyna Cybularczyk,[a,b] Anna Litwińska,[b] Anna Maria Dąbrowska,[a,b] M. Dranka,[c] Grażyna Zofia Żukowska,[c] Mateusz Urbańczyk[a] and Michał Michalak[d]

[a]*Centre of New Technologies, University of Warsaw, Banacha 2c, 02-097, Warsaw, Poland.*

[b]*Faculty of Chemistry, University of Warsaw, Pasteura 1, 02-093, Warsaw, Poland.*

[c]*Faculty of Chemistry, Warsaw University of Technology, Noakowskiego 3, 00-664, Warsaw, Poland.*

[d]*Institute of Organic Chemistry, Polish Academy of Science, Kasprzaka 44/52, 01-224, Warsaw, Poland.*

1) ^{1}H and ^{13}C NMR Data

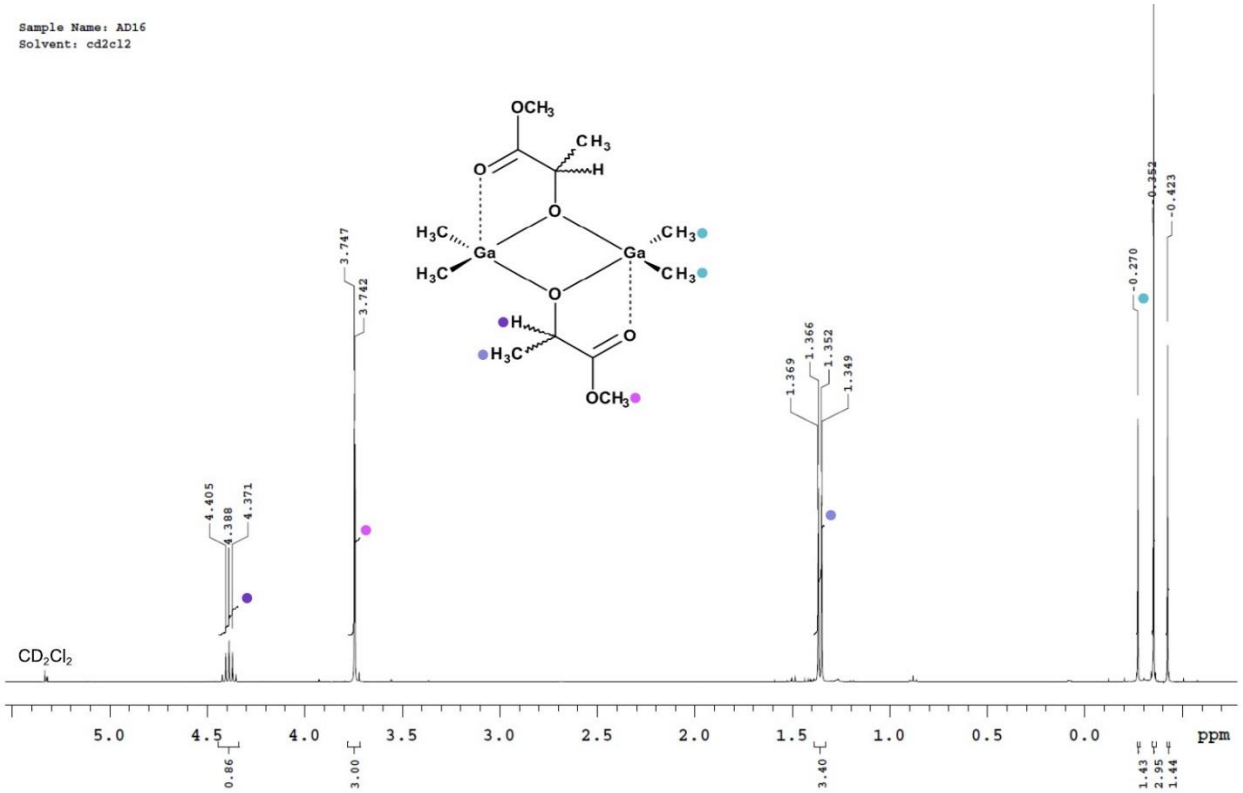

Figure S1. ^{1}H NMR (CD_2Cl_2, 400 MHz) spectrum of (*R*,*S*)-**1**.

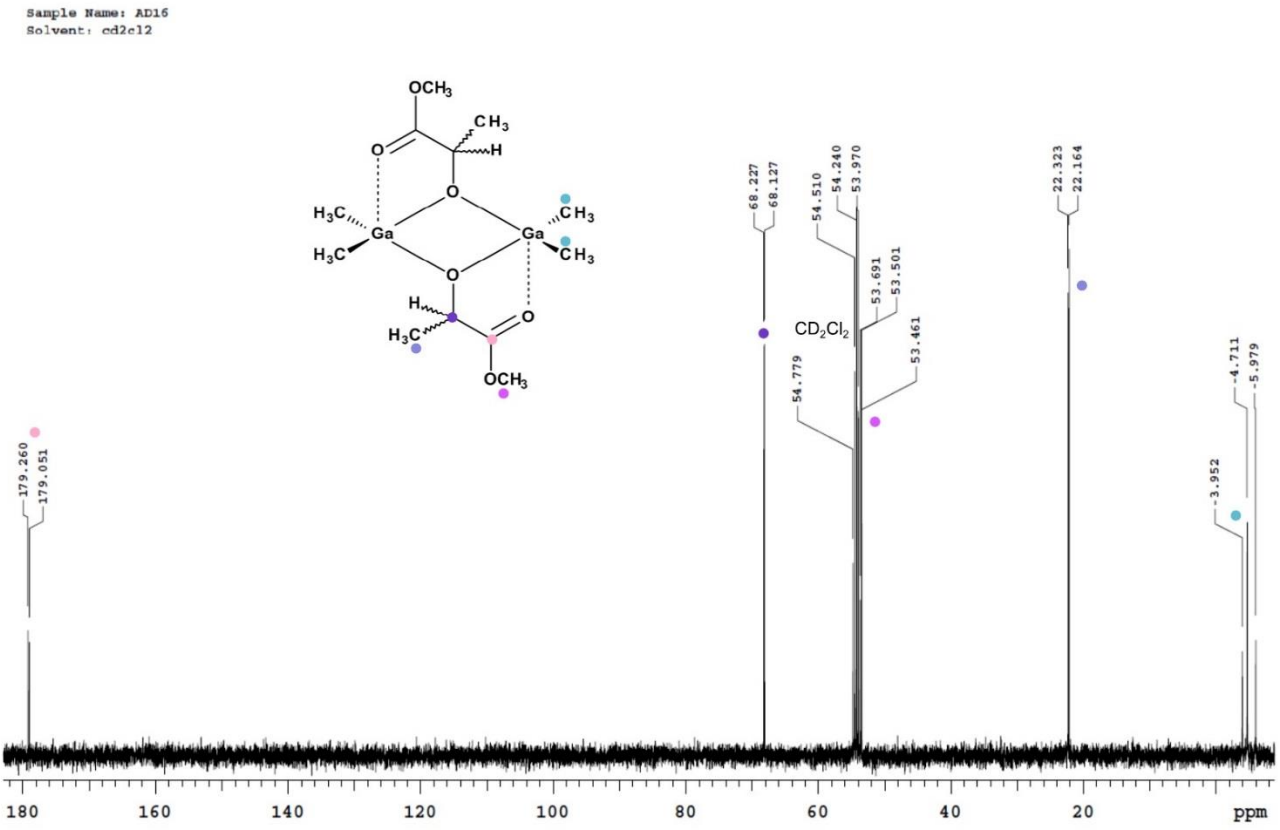

Figure S2. ^{13}C NMR (CD_2Cl_2, 100 MHz) spectrum of (*R*,*S*)-**1**.

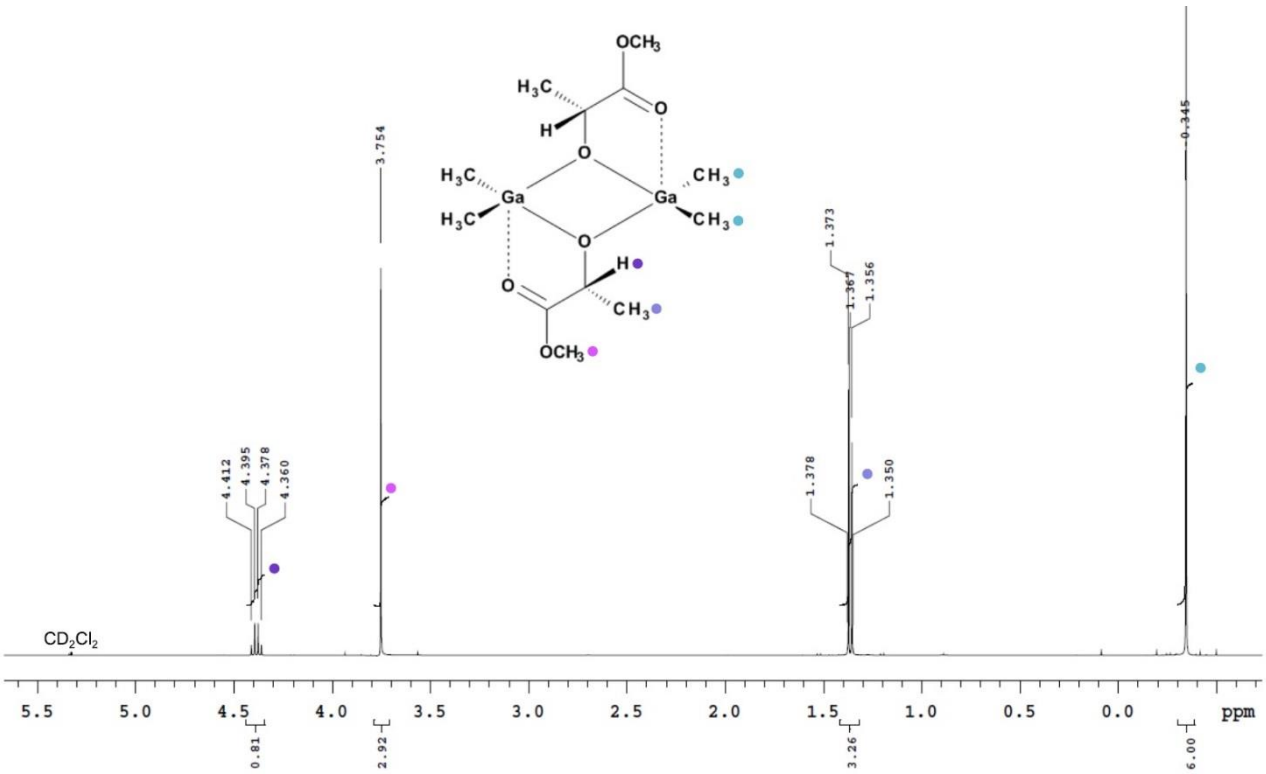

Figure S3. ^{1}H NMR (CD_2Cl_2, 400 MHz) spectrum of (*R,R)*-**1**.

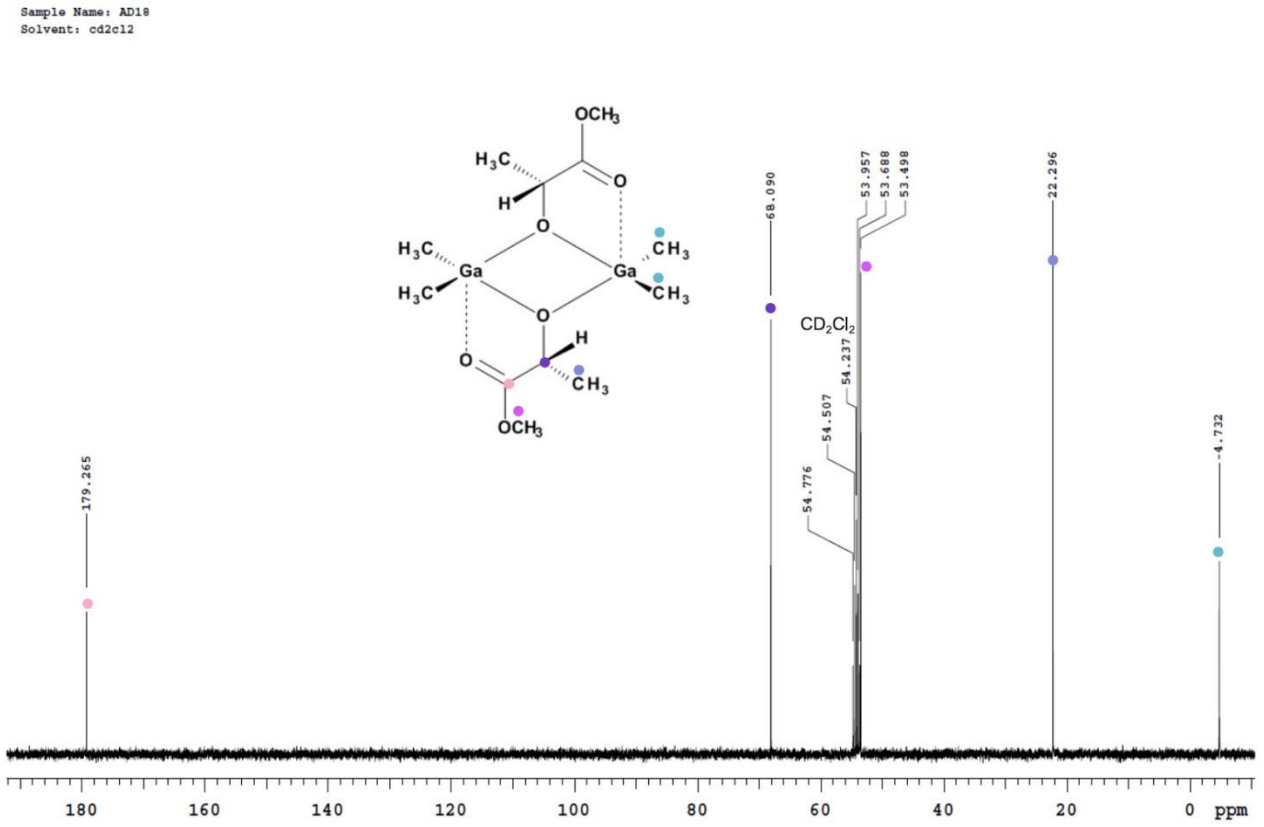

Figure S4. ^{13}C NMR (CD_2Cl_2, 100 MHz) spectrum of (*R,R)*-**1**.

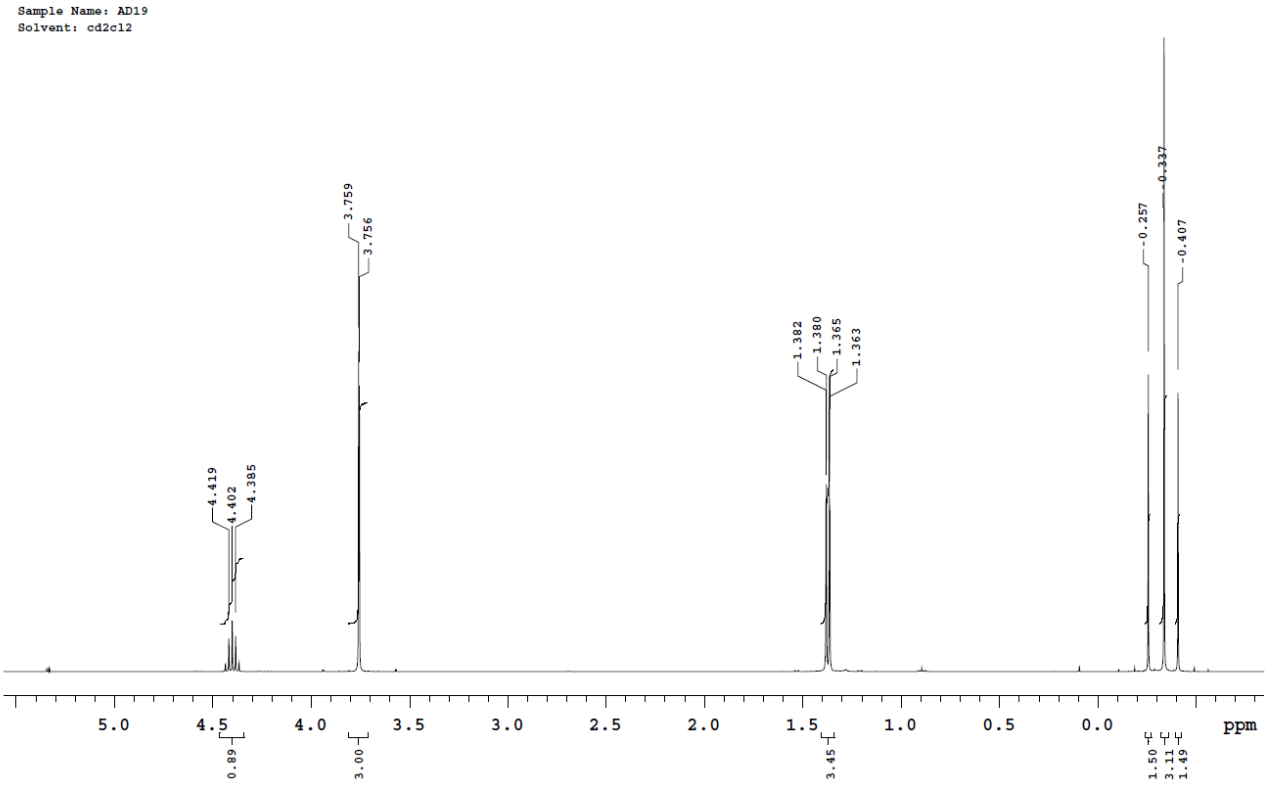

Figure S5. ^{1}H NMR (CD_2Cl_2, 400 MHz) spectrum of the mixture of *(R,R)*-**1** and *(S,S)*-**1**.

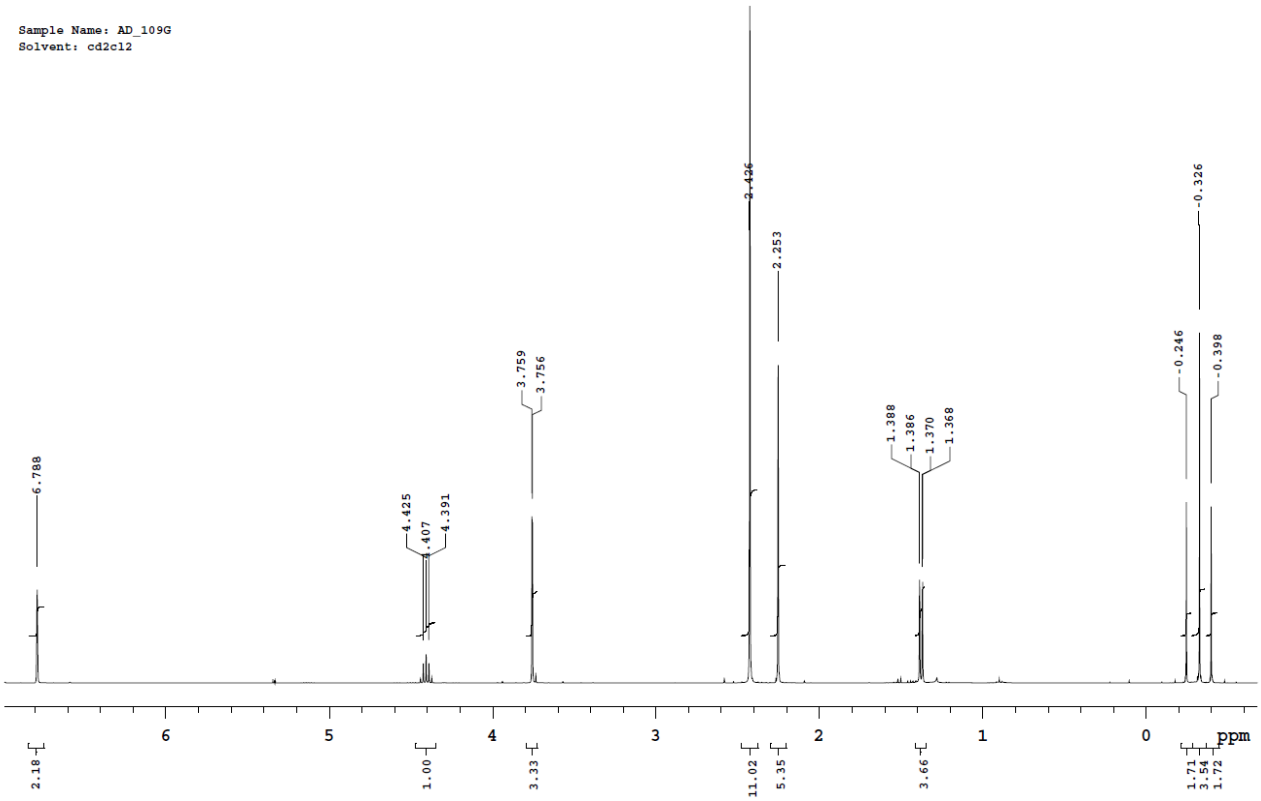

Figure S6. ^{1}H NMR (CD_2Cl_2, 400 MHz) spectrum of **1**/2,4,6-collidine (1:6).

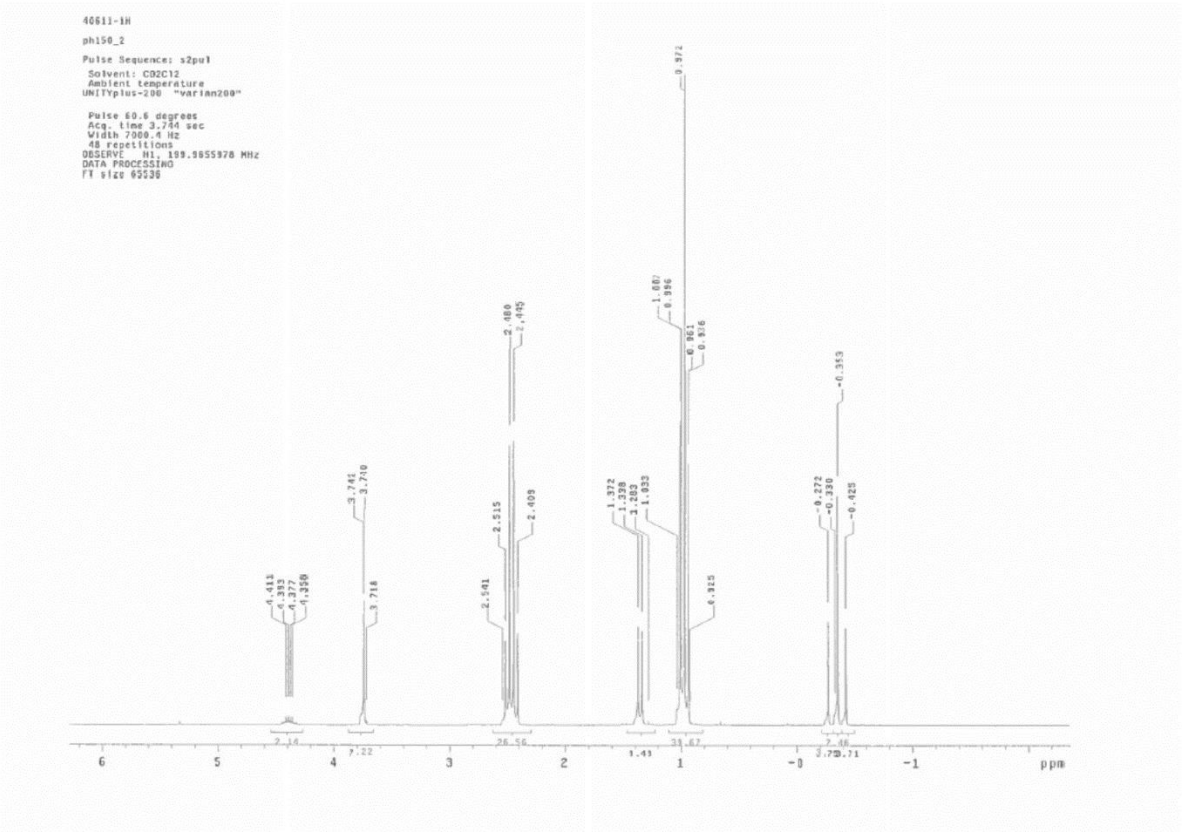

Figure S7. ^{1}H NMR (CD_2Cl_2, 200 MHz) spectrum of **1**/TEA (1:6).

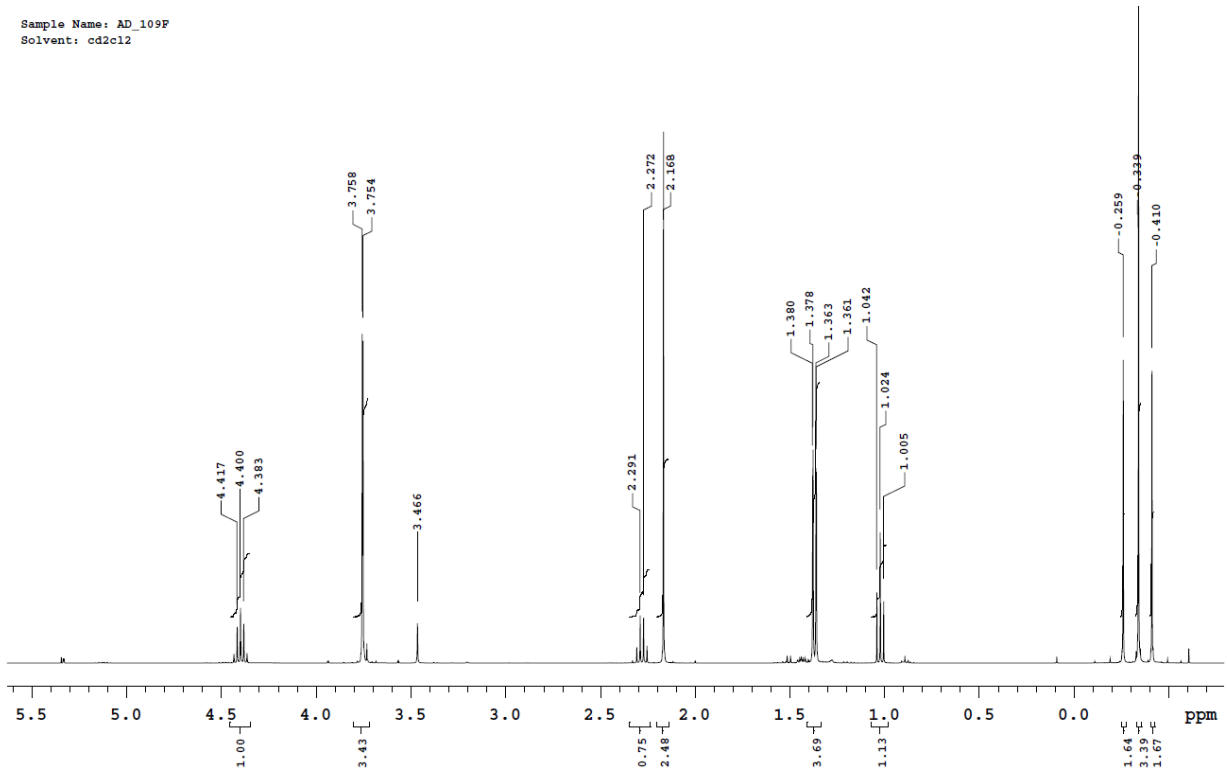

Figure S8. ^{1}H NMR (CD_2Cl_2, 400 MHz) spectrum of **1**/DMEA (1:6).

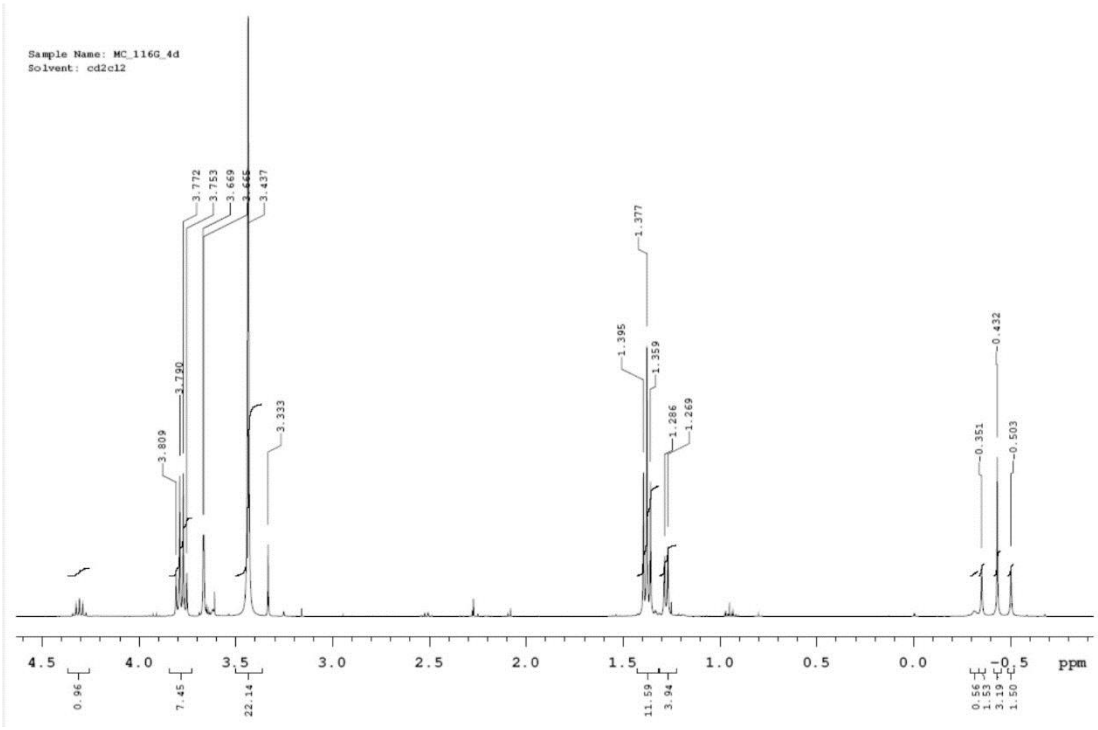

Figure S9. ^{1}H NMR (CD_2Cl_2, 400 MHz) spectrum of **1**/DMEA (1:6) (after 4 days at 40°C).

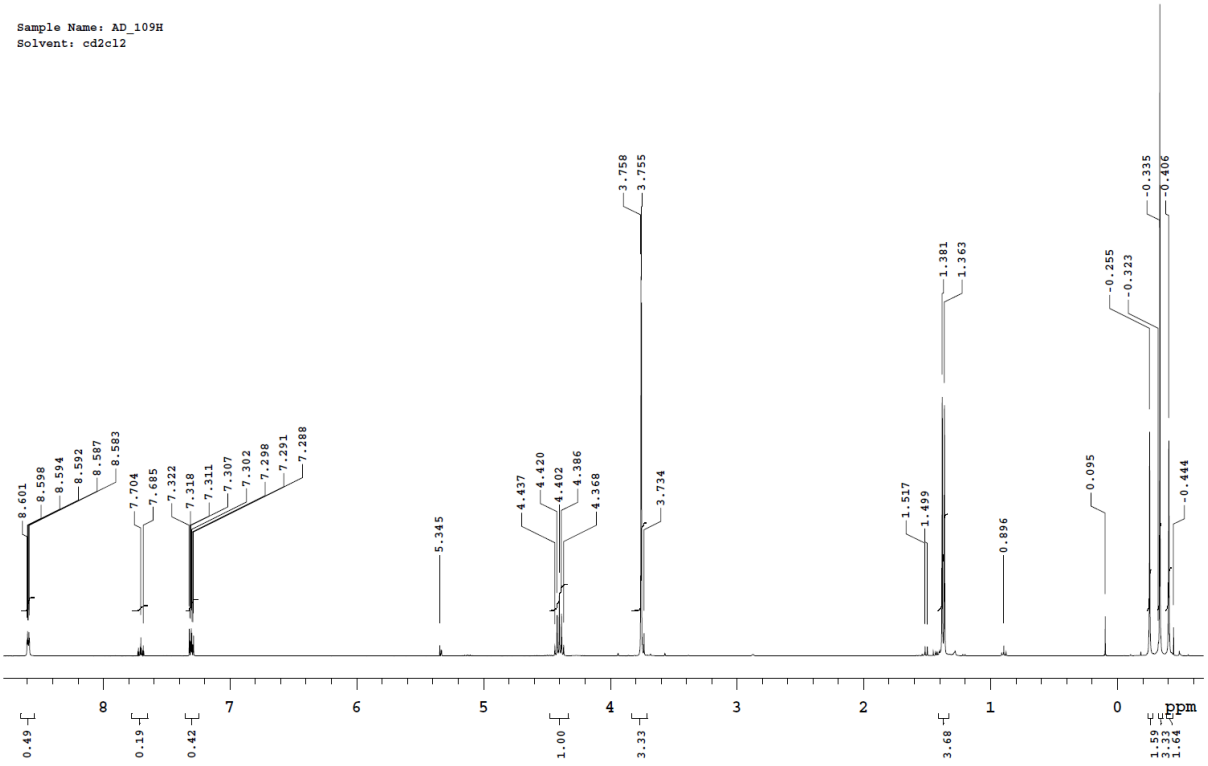

Figure S10. ^{1}H NMR (CD_2Cl_2, 400 MHz) spectrum of **1**/pyridine (1:1).

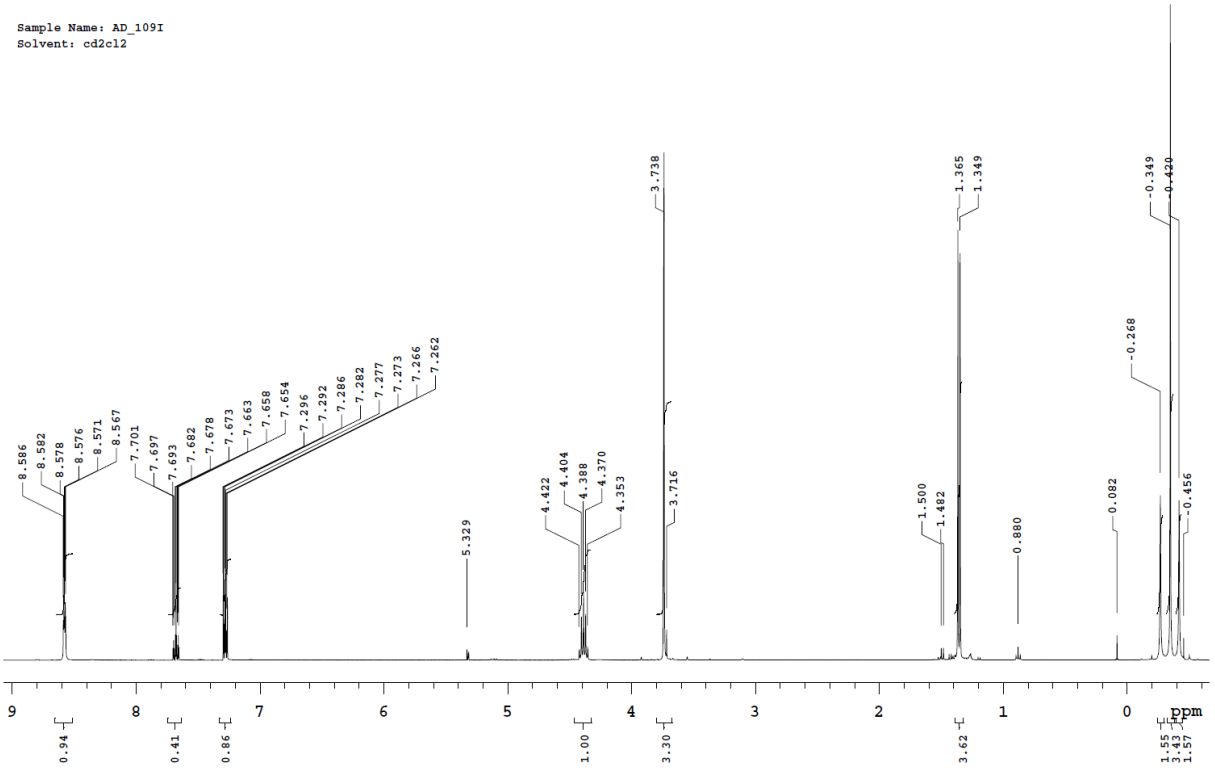

Figure S11. ^{1}H NMR (CD_2Cl_2, 400 MHz) spectrum of **1**/pyridine (1:2).

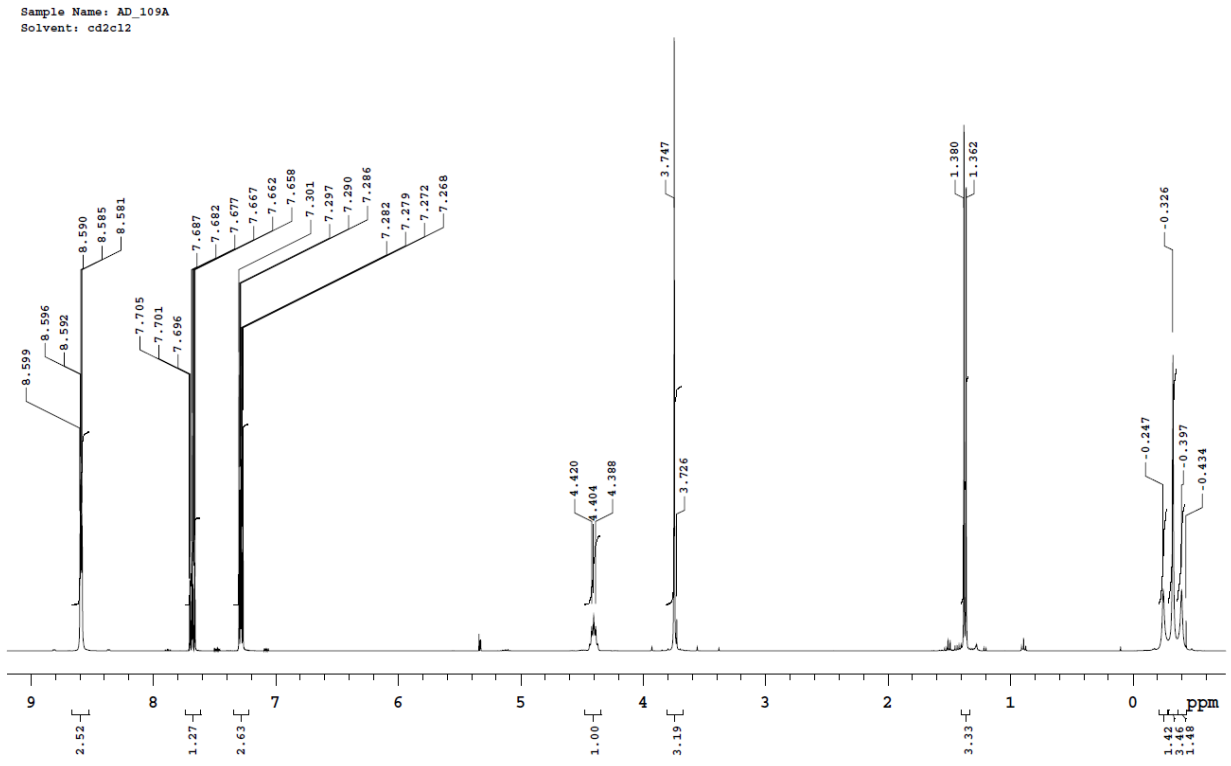

Figure S12. ^{1}H NMR (CD_2Cl_2, 400 MHz) spectrum of **1**/pyridine (1:6).

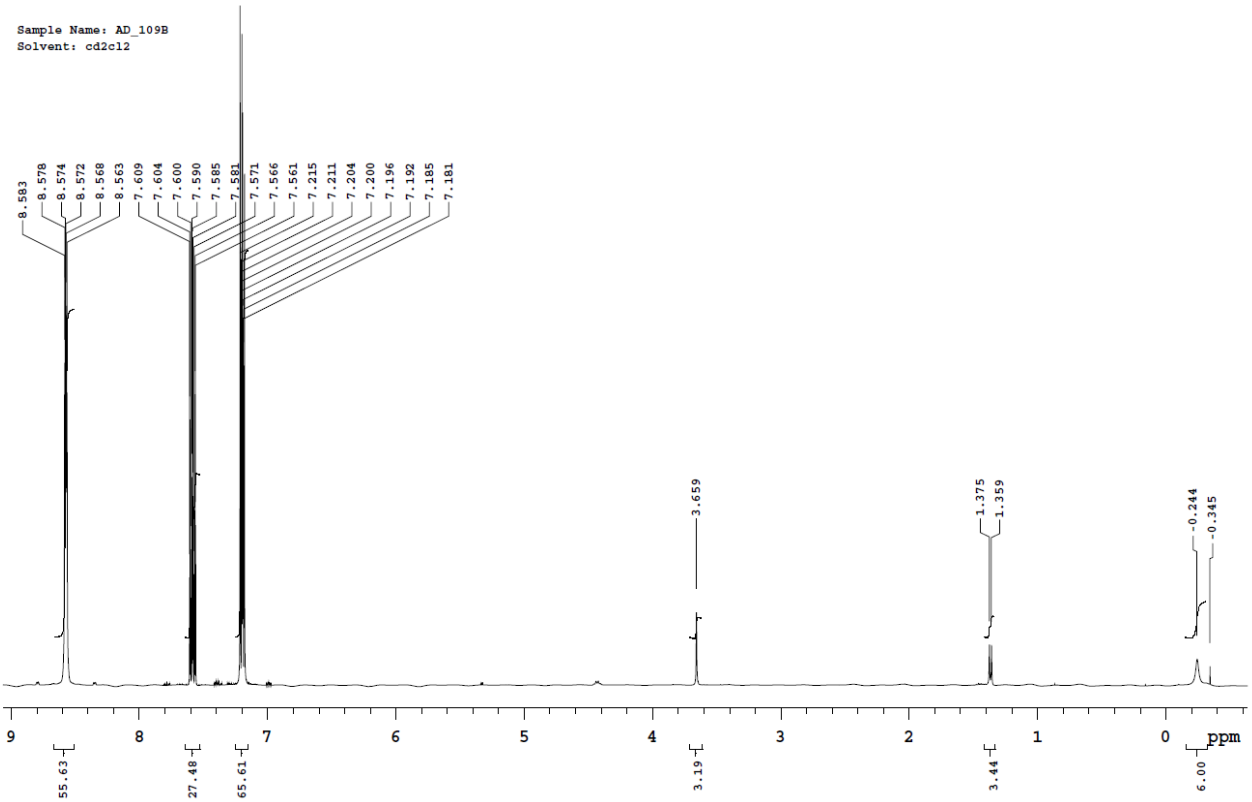

Figure S13. ^{1}H NMR (CD_2Cl_2, 400 MHz) spectrum of **1**/pyridine (1:60).

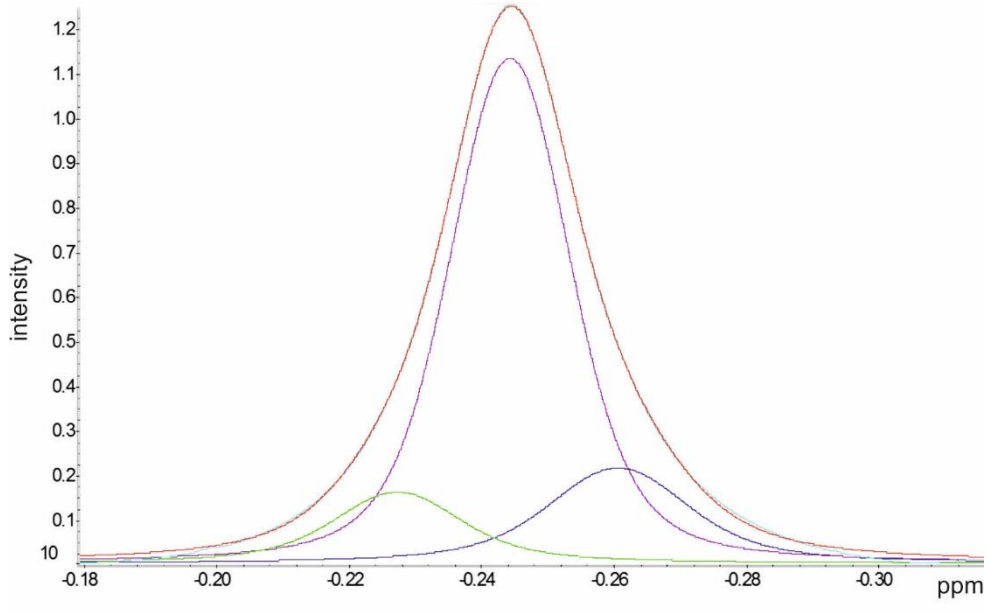

Figure S14. ^{1}H NMR (CD_2Cl_2, 400 MHz) spectrum of **1**/pyridine (1:60) - deconvolution of the signal corresponding to Ga-Me protons (–0.261 - area 71986.6953, –0.244 - area 299951.7188, –0.227 - area 49406.2695.

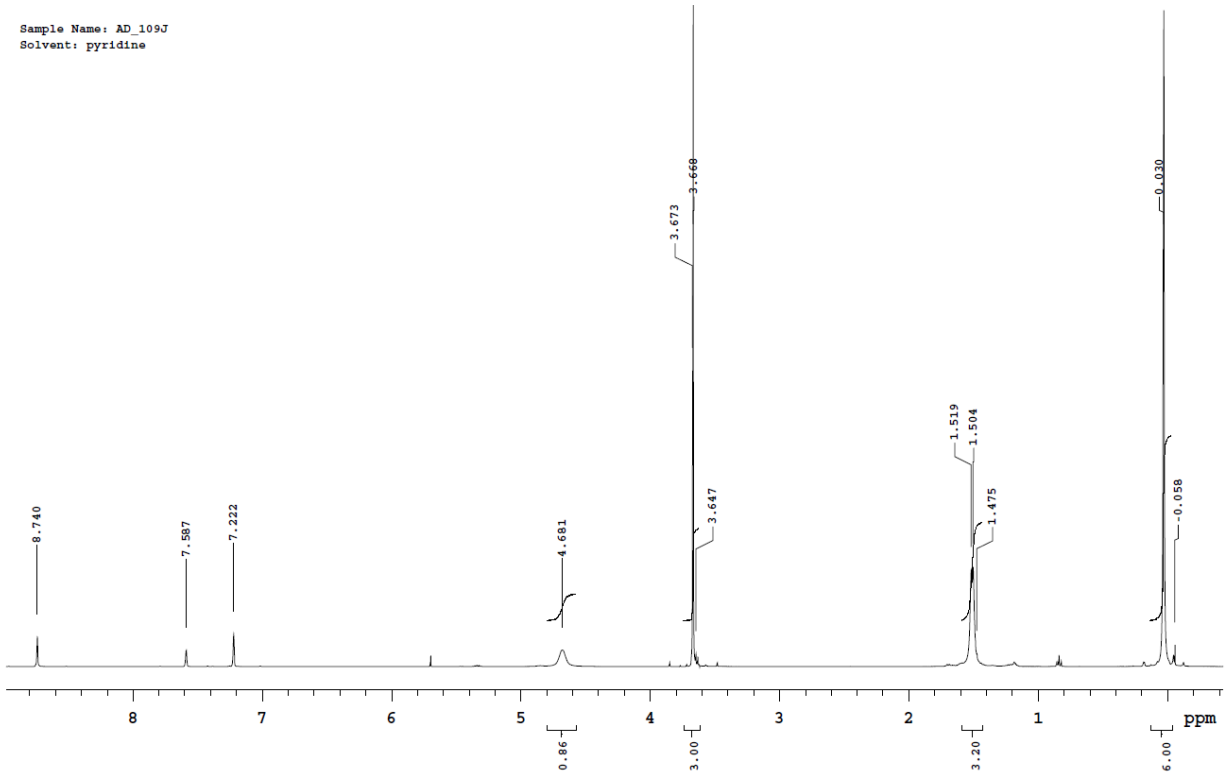

Figure S15. ^{1}H NMR (pyridine-d_5, 400 MHz) spectrum of **1** .

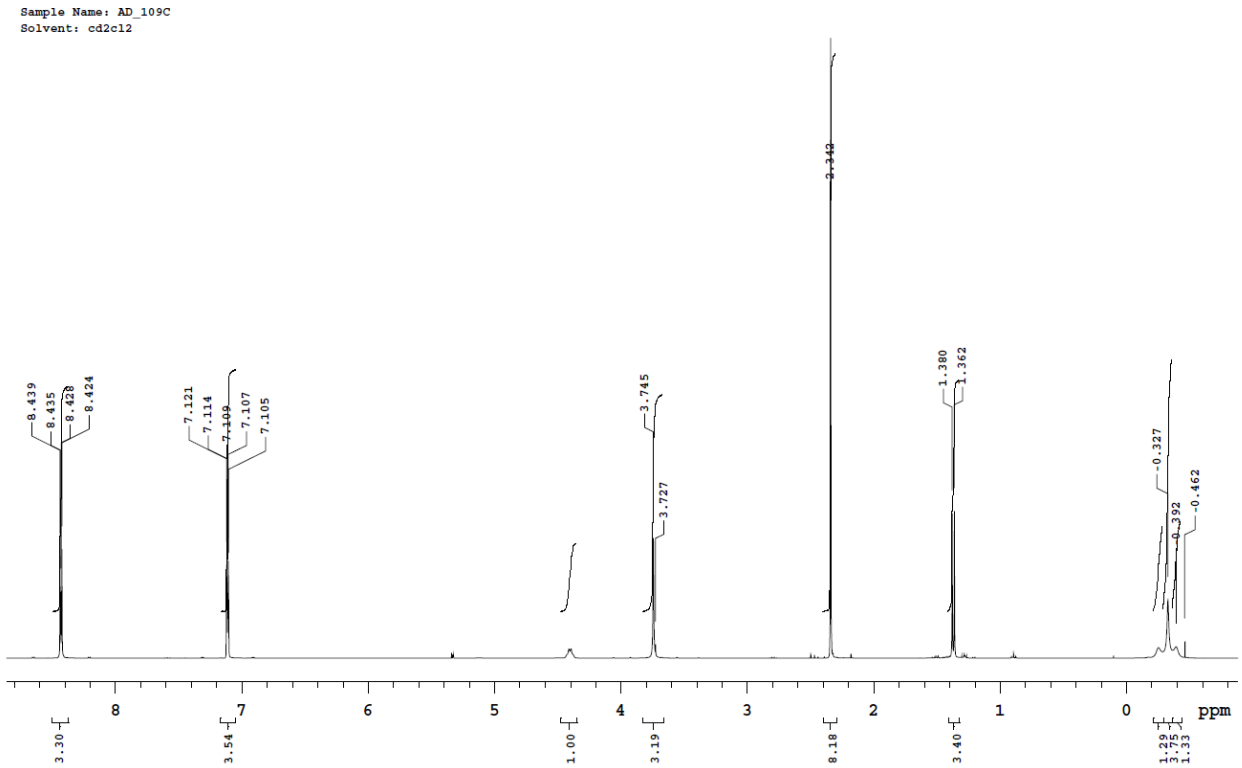

Figure S16. ^{1}H NMR (CD_2Cl_2, 400 MHz) spectrum of **1**/γ-picoline (1:6).

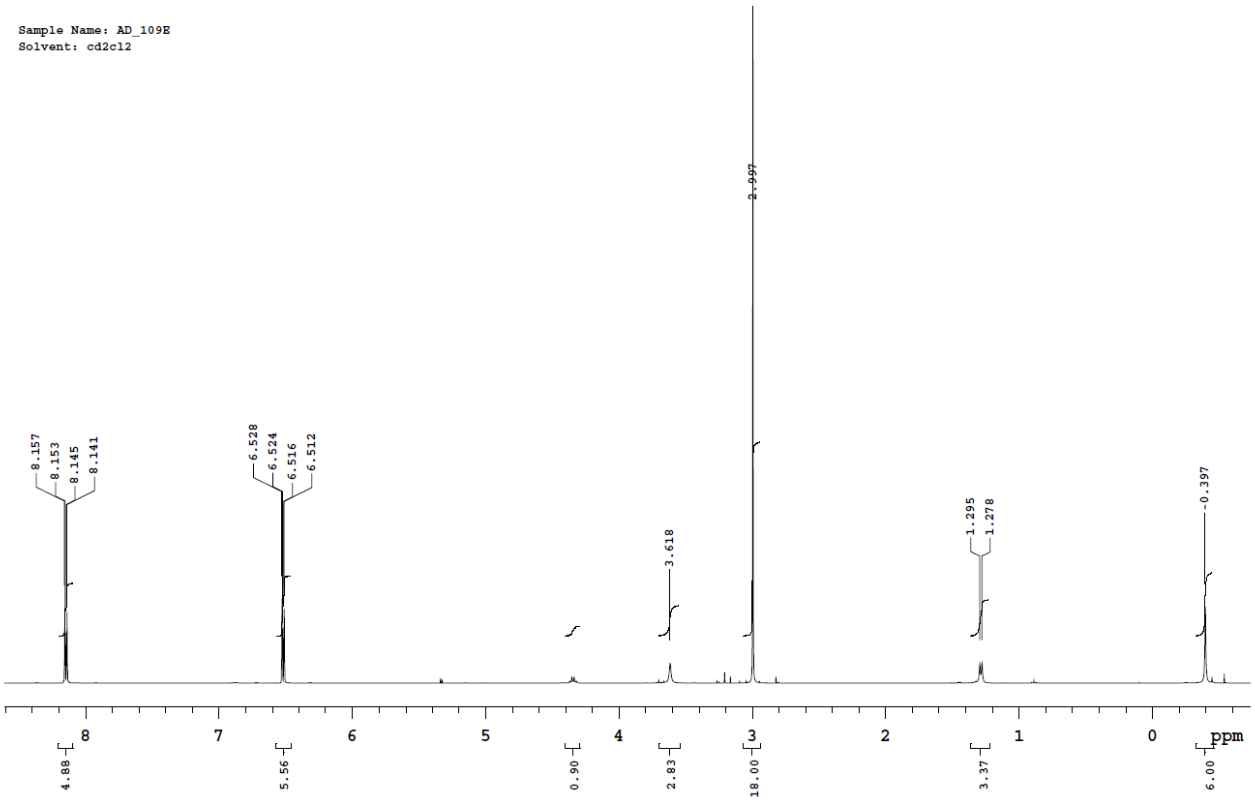

Figure S17. ^{1}H NMR (CD_2Cl_2, 400 MHz) spectrum of **1**/DMAP (1:6).

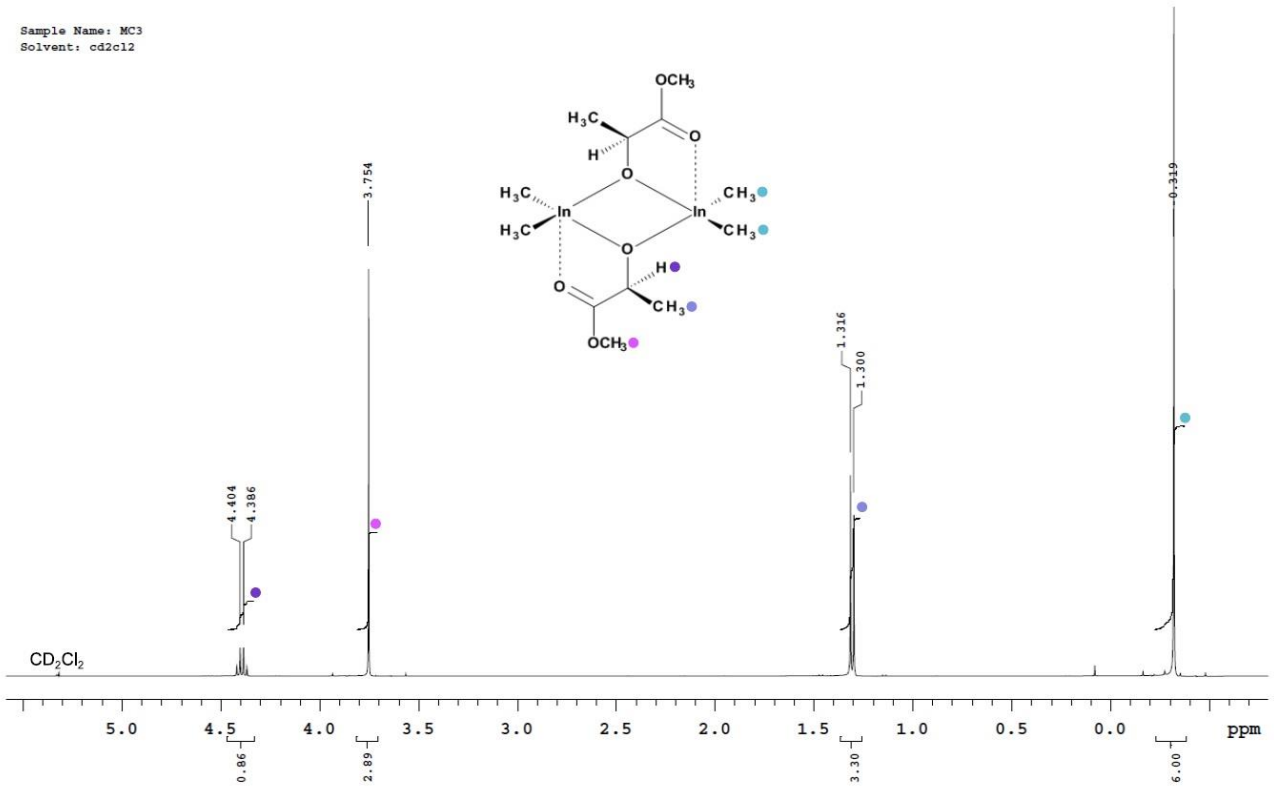

Figure S18. ^{1}H NMR (CD_2Cl_2, 400 MHz) spectrum of (*S*,*S*)-**2**.

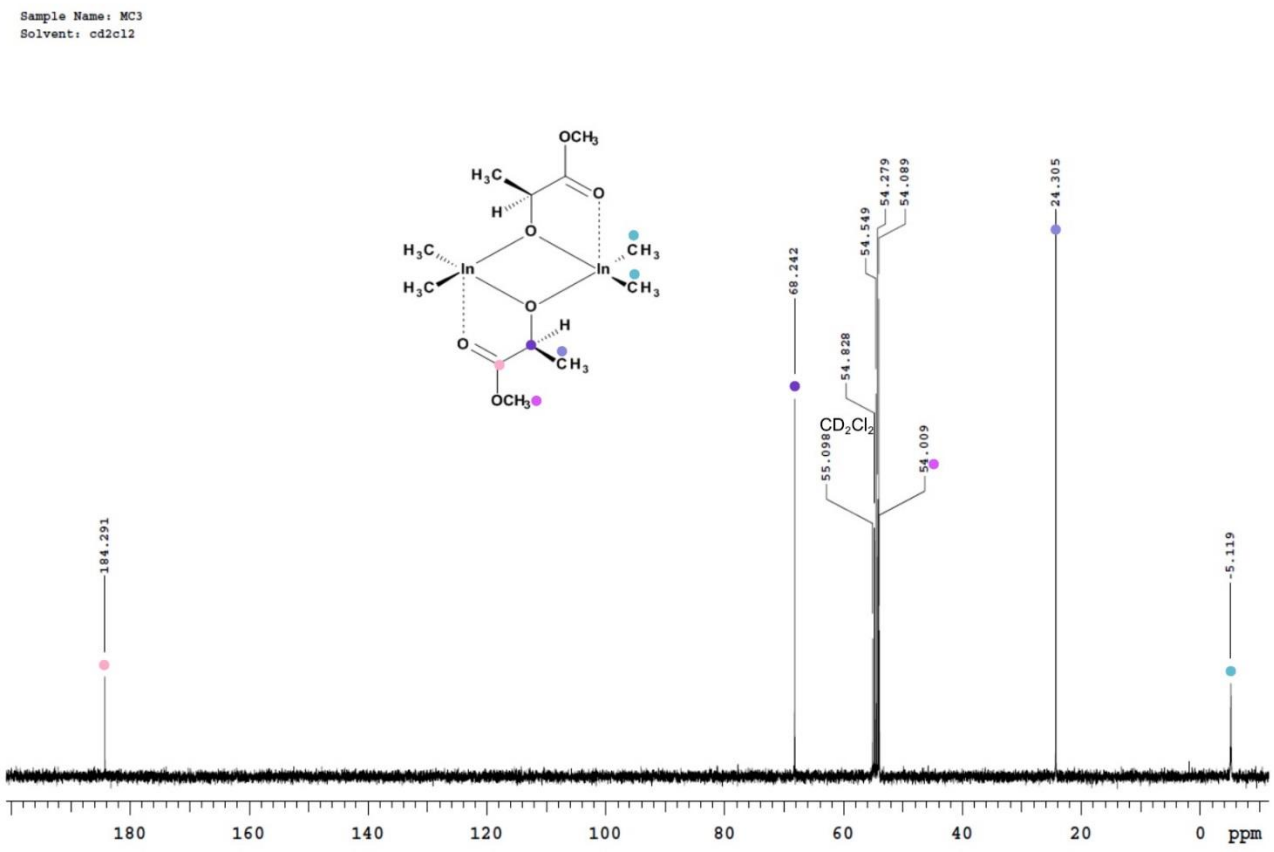

Figure S19. ^{13}C NMR (CD_2Cl_2, 100 MHz) spectrum of (*S*,*S*)-**2**.

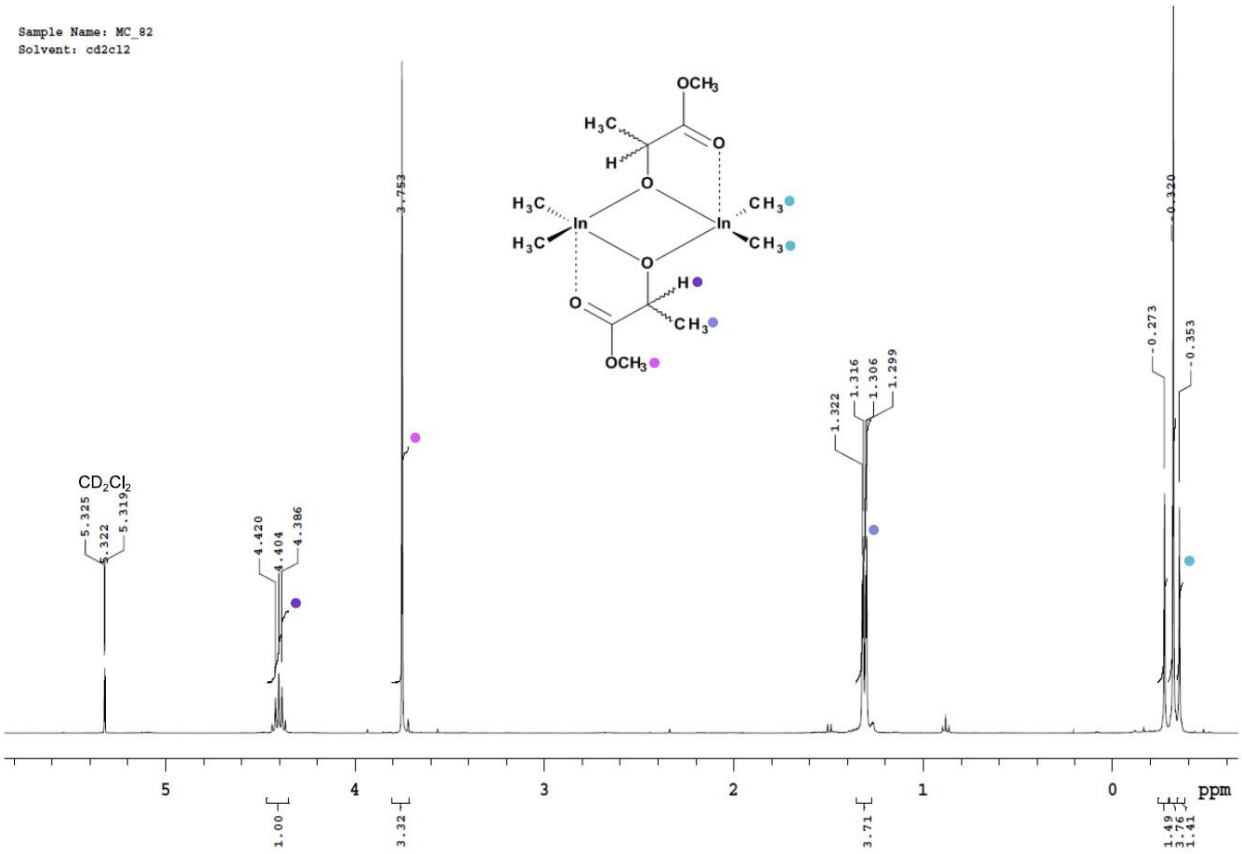

Figure S20. ^{1}H NMR (CD_2Cl_2, 400 MHz) spectrum of **2**.

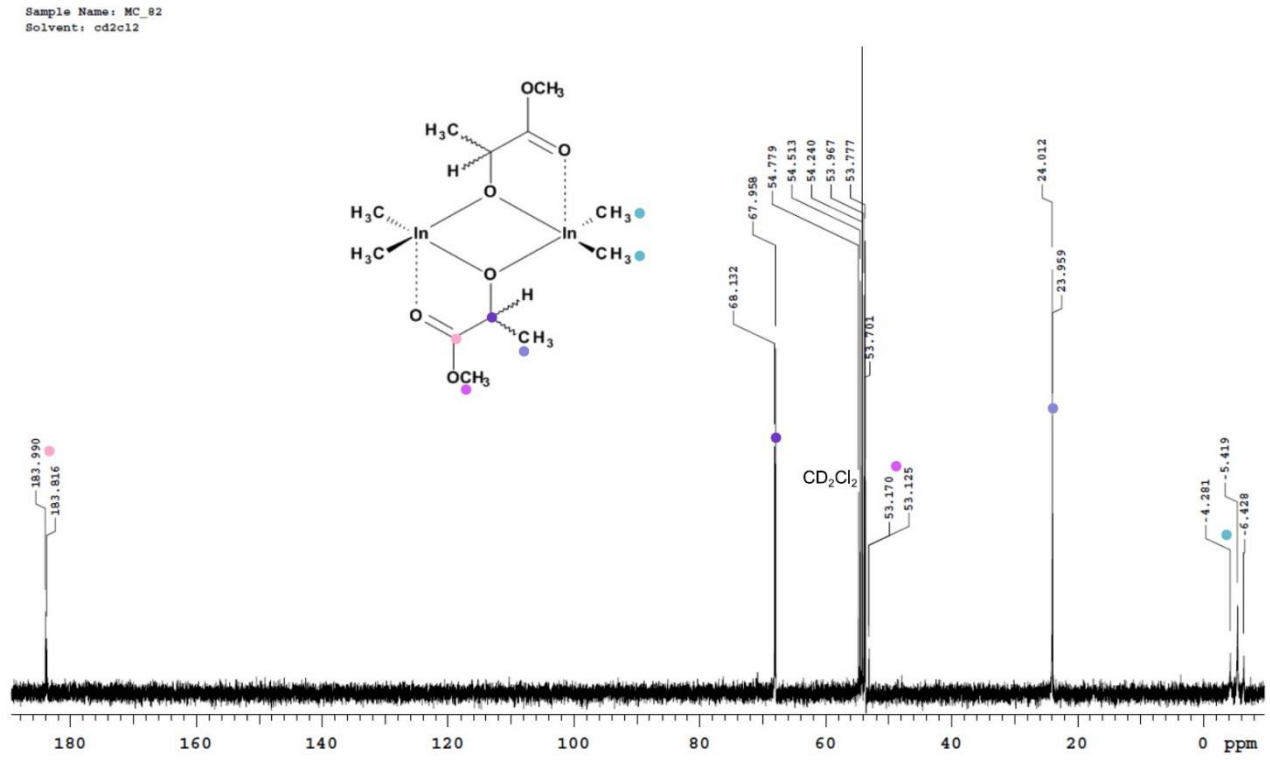

Figure S21. ^{13}C NMR (CD_2Cl_2, 100 MHz) spectrum of **2**.

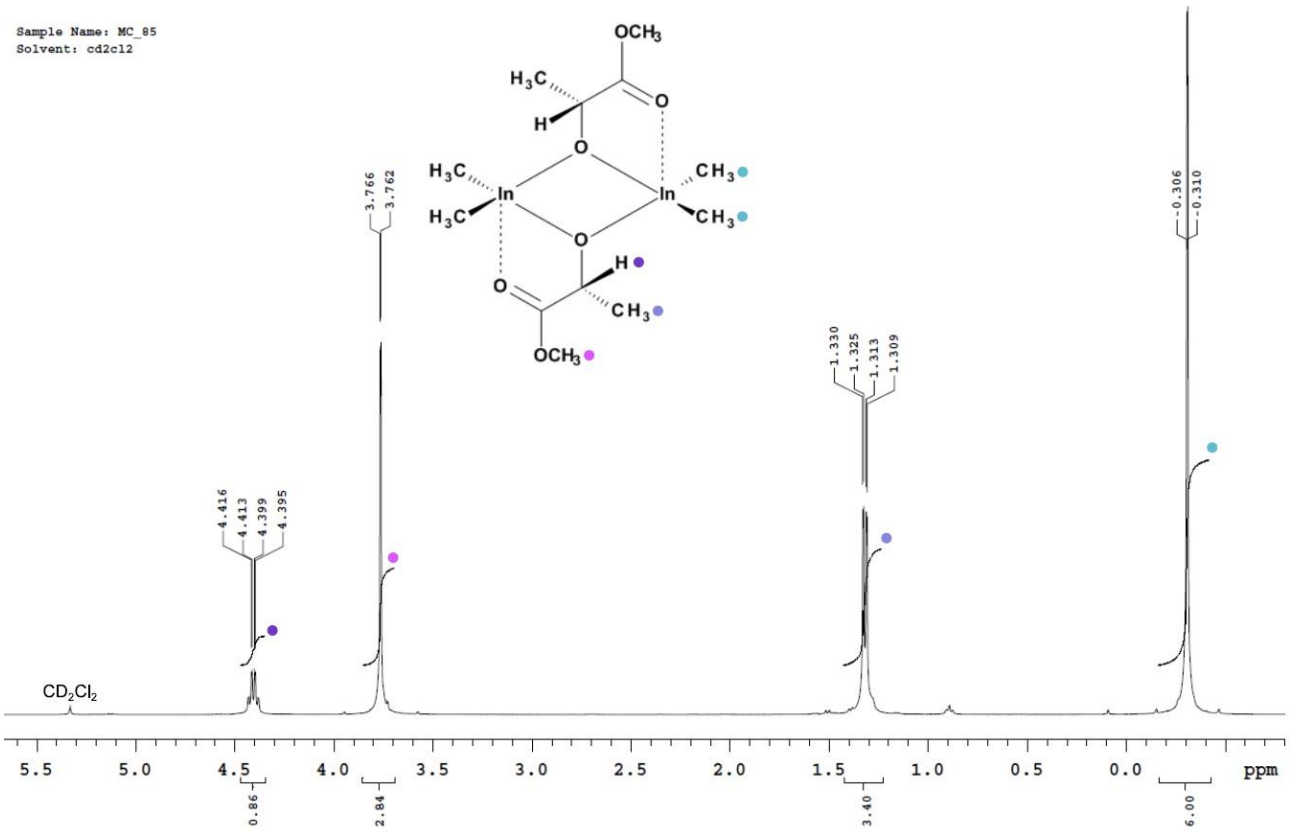

Figure S22. ^{1}H NMR (CD_2Cl_2, 400 MHz) spectrum of (*R*,*R*)-**2**.

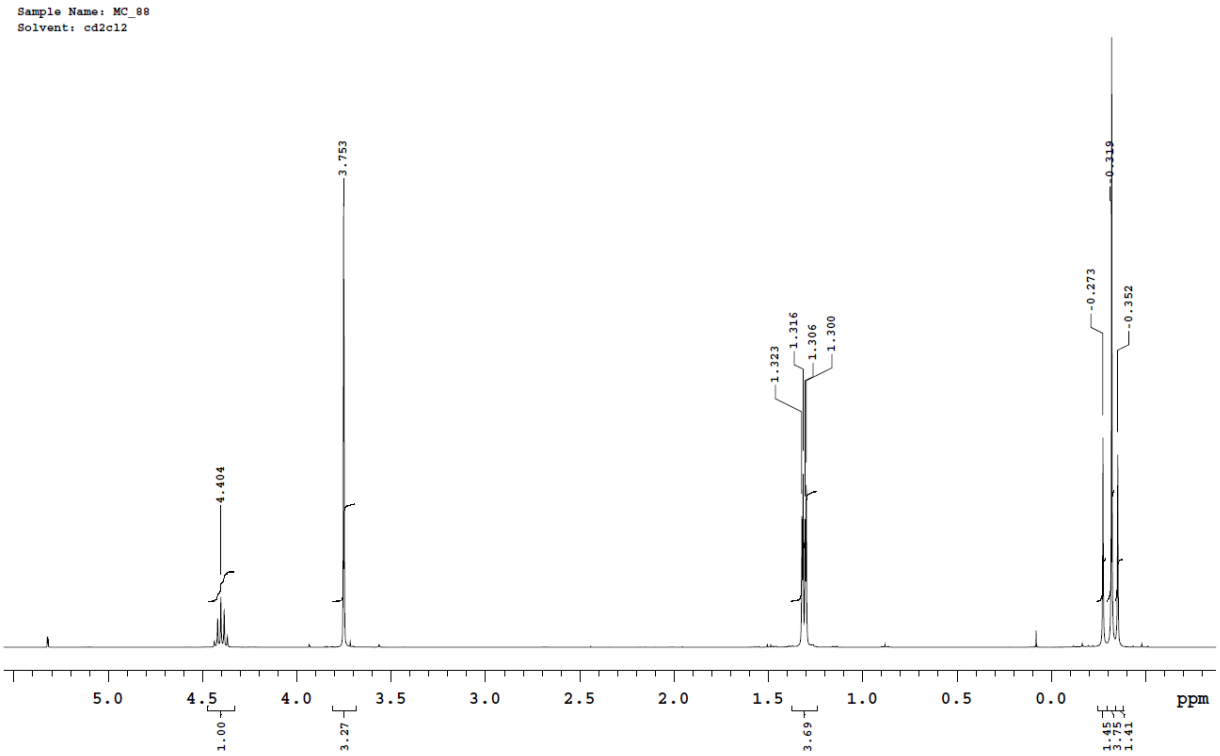

Figure S23. ^{1}H NMR (CD_2Cl_2, 400 MHz) spectrum of the mixture of (*R*,*R*)-**2** and (*S*,*S*)-**2**.

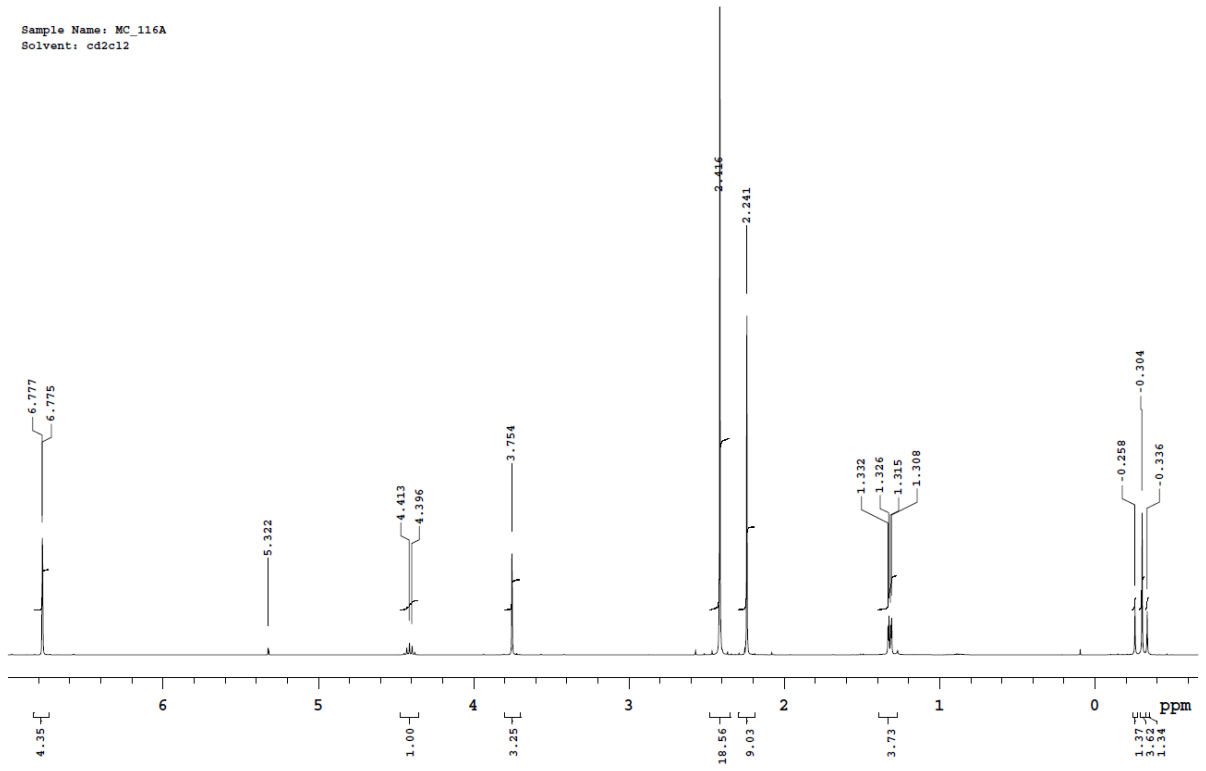

Figure S24. ^{1}H NMR (CD_2Cl_2, 400 MHz) spectrum of **2**/2,4,6-collidine (1:6)

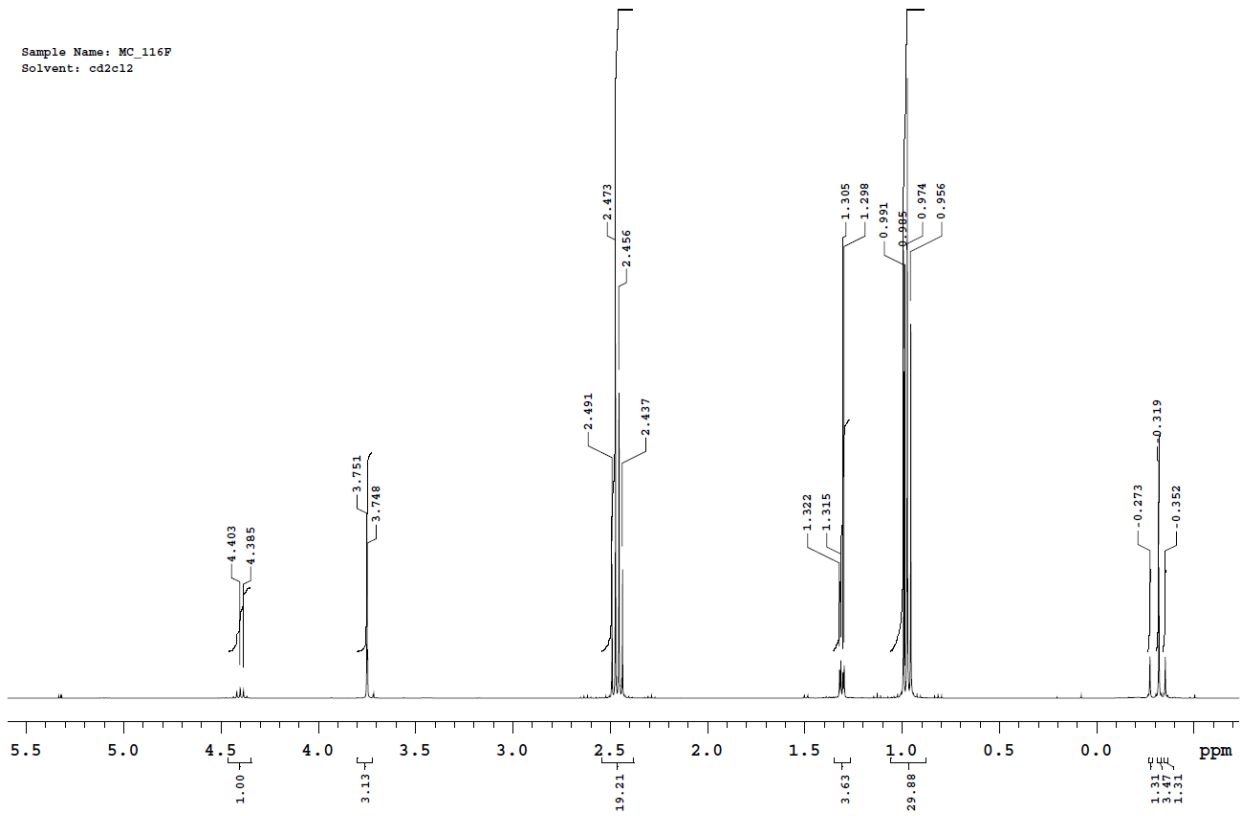

Figure S25. ^{1}H NMR (CD_2Cl_2, 400 MHz) spectrum of **2**/TEA (1:6).

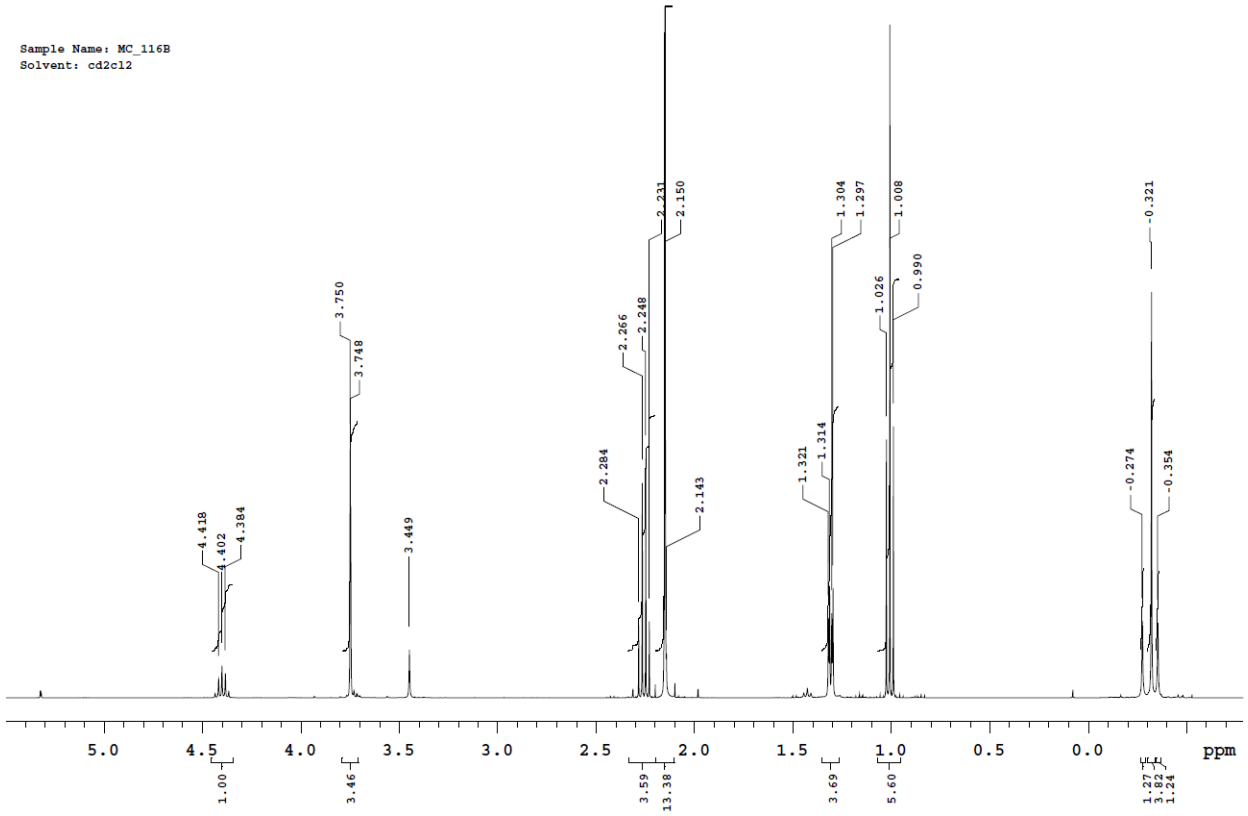

Figure S26. ^{1}H NMR (CD_2Cl_2, 400 MHz) spectrum of **2**/DMEA (1:6).

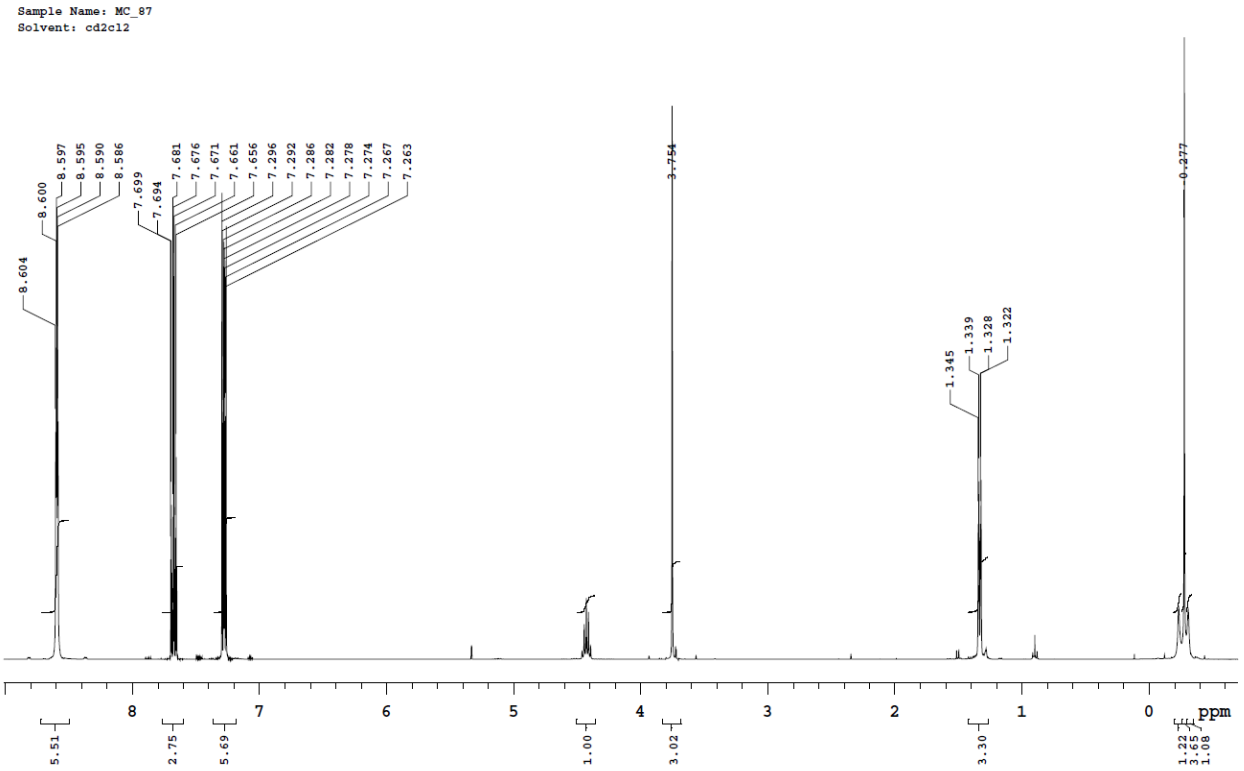

Figure S27. ^{1}H NMR (CD_2Cl_2, 400 MHz) spectrum of **2**/pyridine (1:6).

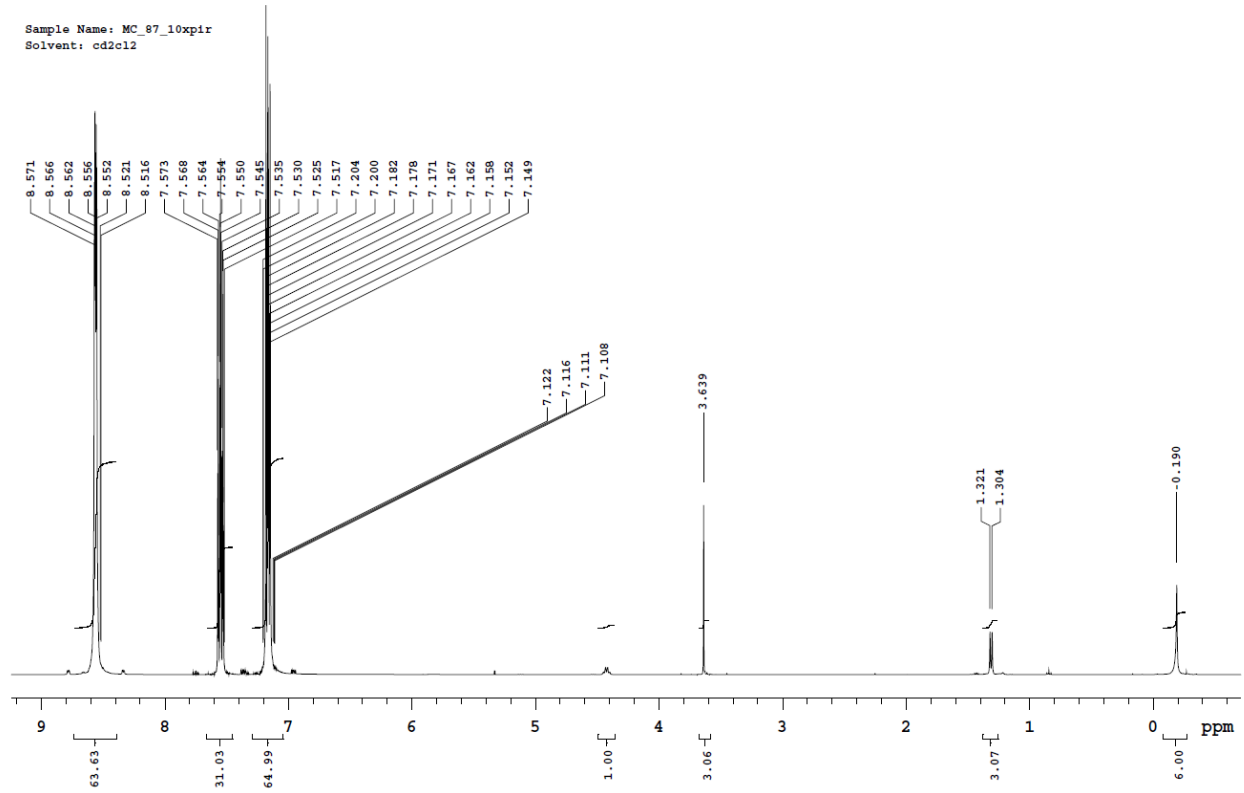

Figure S28. ^{1}H NMR (CD_2Cl_2, 400 MHz) spectrum of **2**/pyridine (1:60).

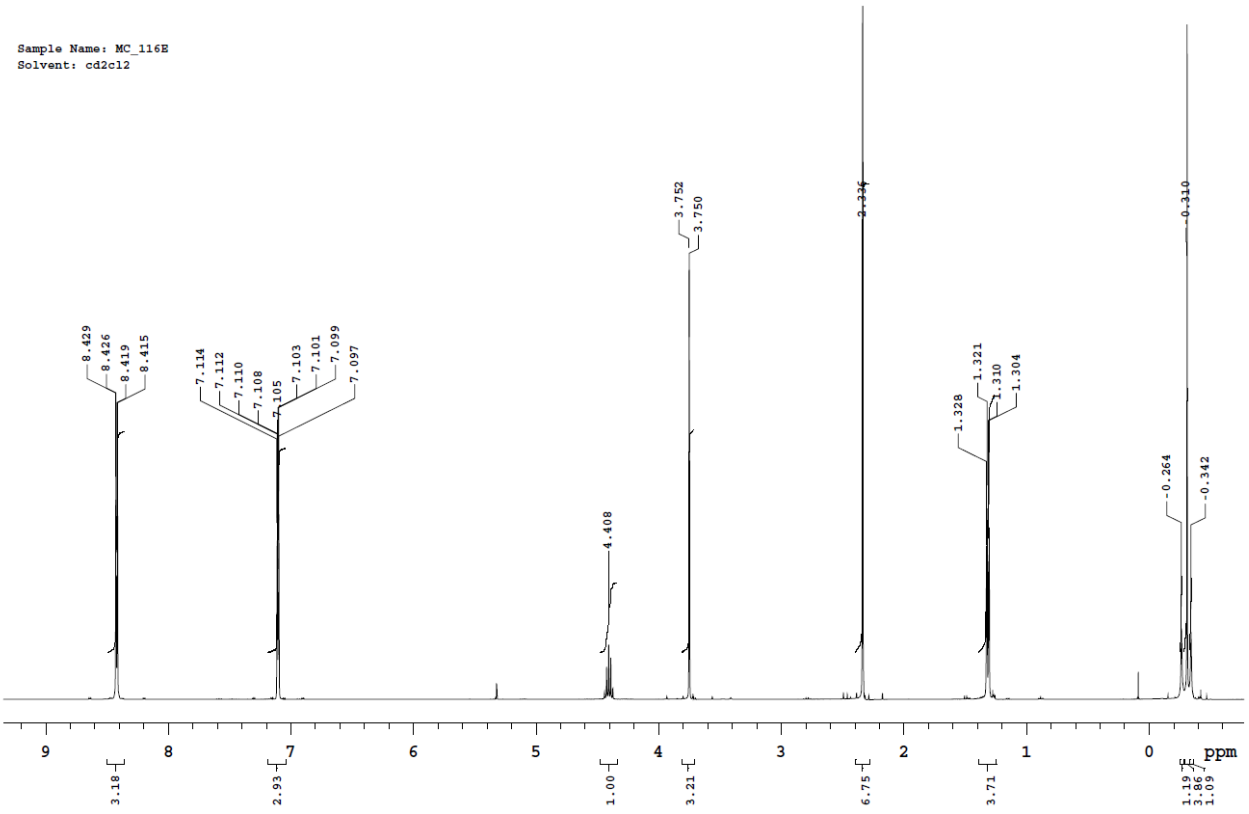

Figure S29. ^{1}H NMR (CD_2Cl_2, 400 MHz) spectrum of **2**/γ-picoline (1:6).

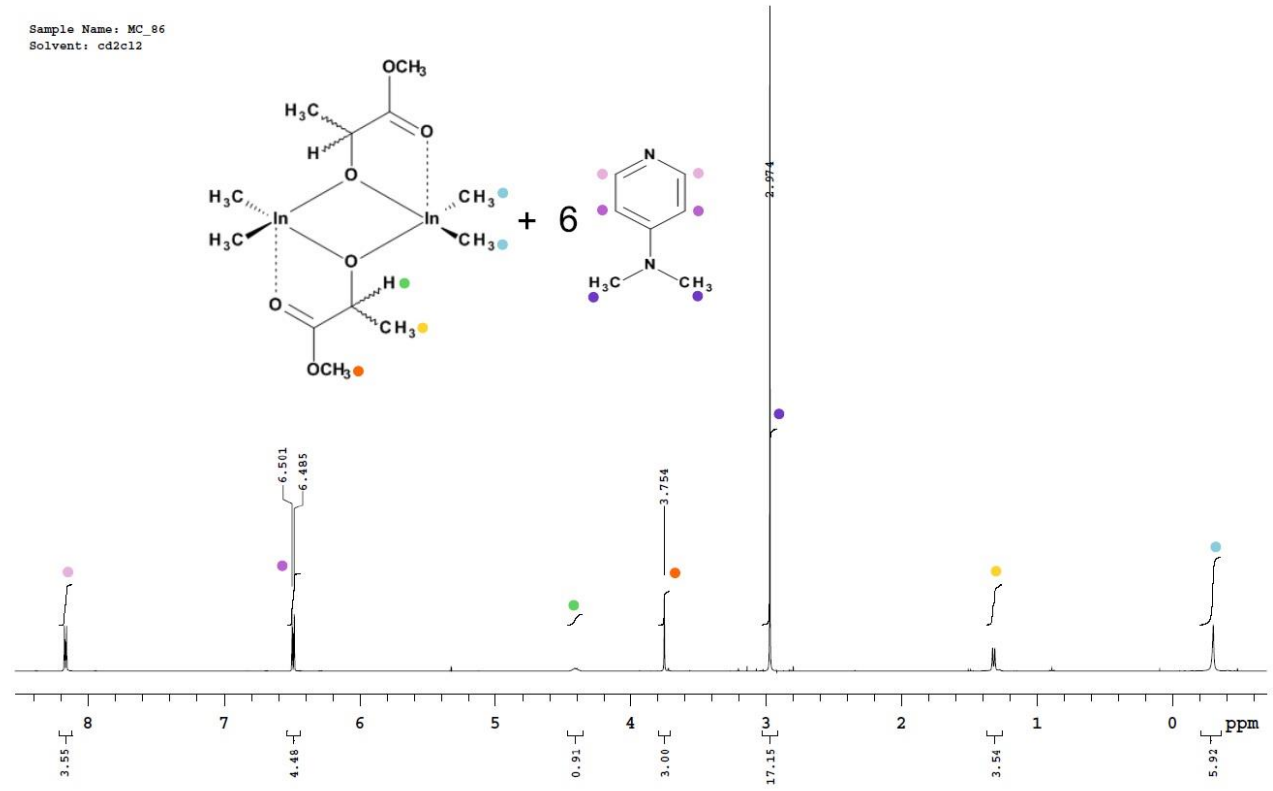

Figure S30. ^{1}H NMR (CD_2Cl_2, 400 MHz) spectrum of **2**/DMAP (1:6).

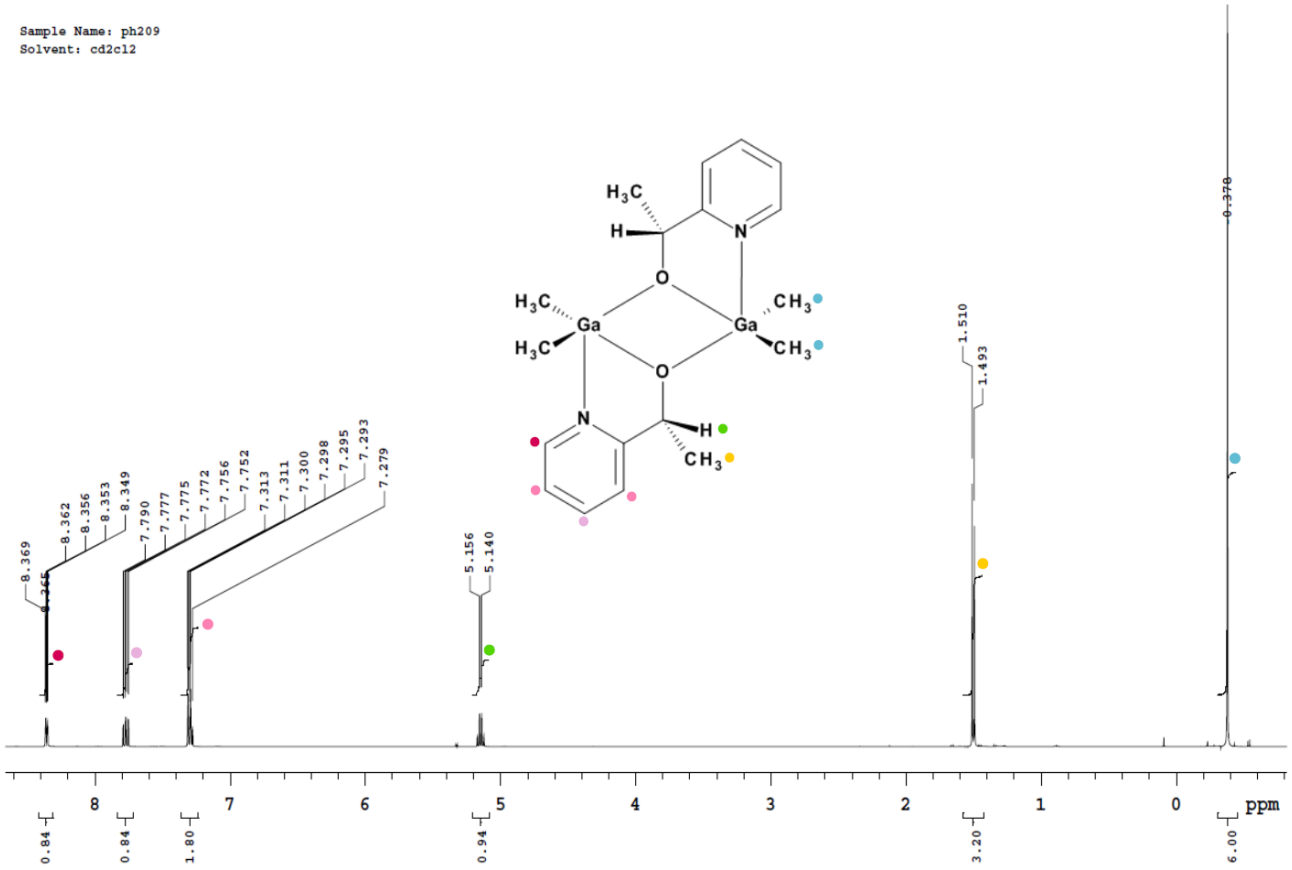

Figure S31. ^{1}H NMR (CD_2Cl_2, 400 MHz) spectrum of **3**.

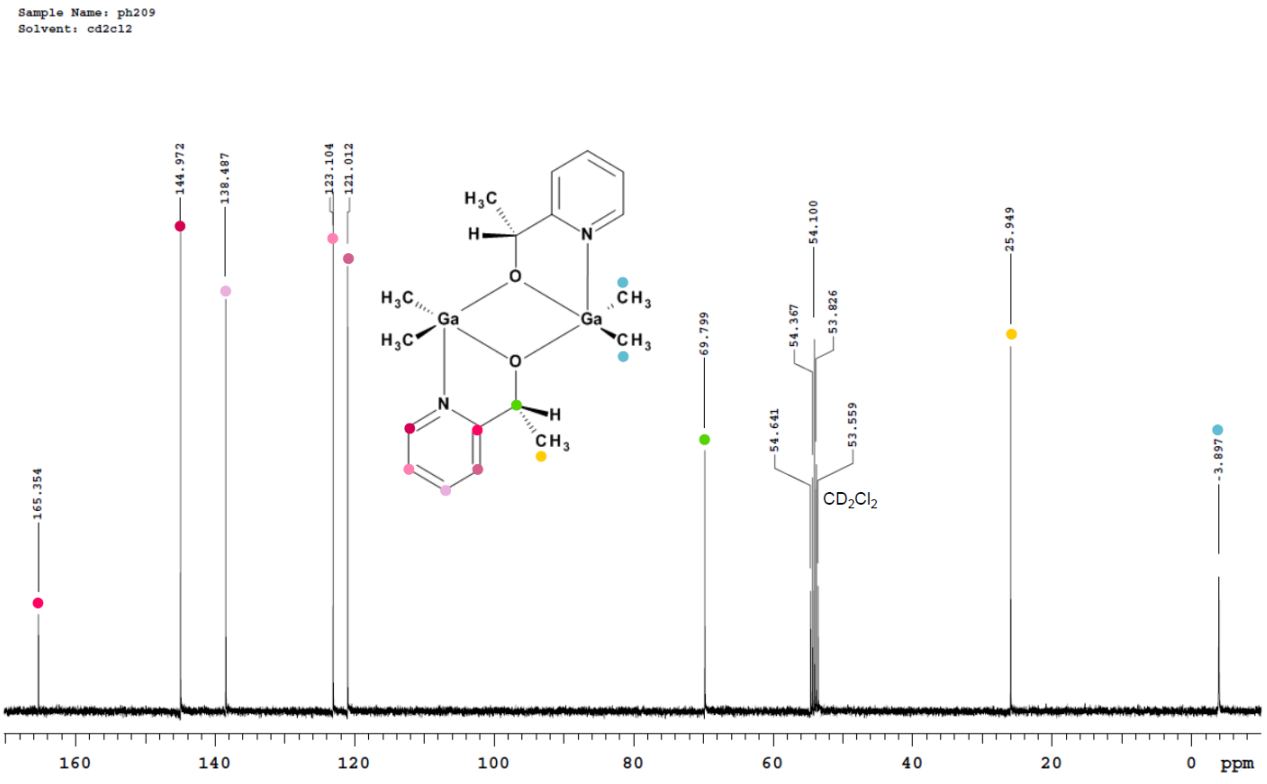

Figure S32. ^{13}C NMR (CD_2Cl_2, 100 MHz) spectrum of **3**.

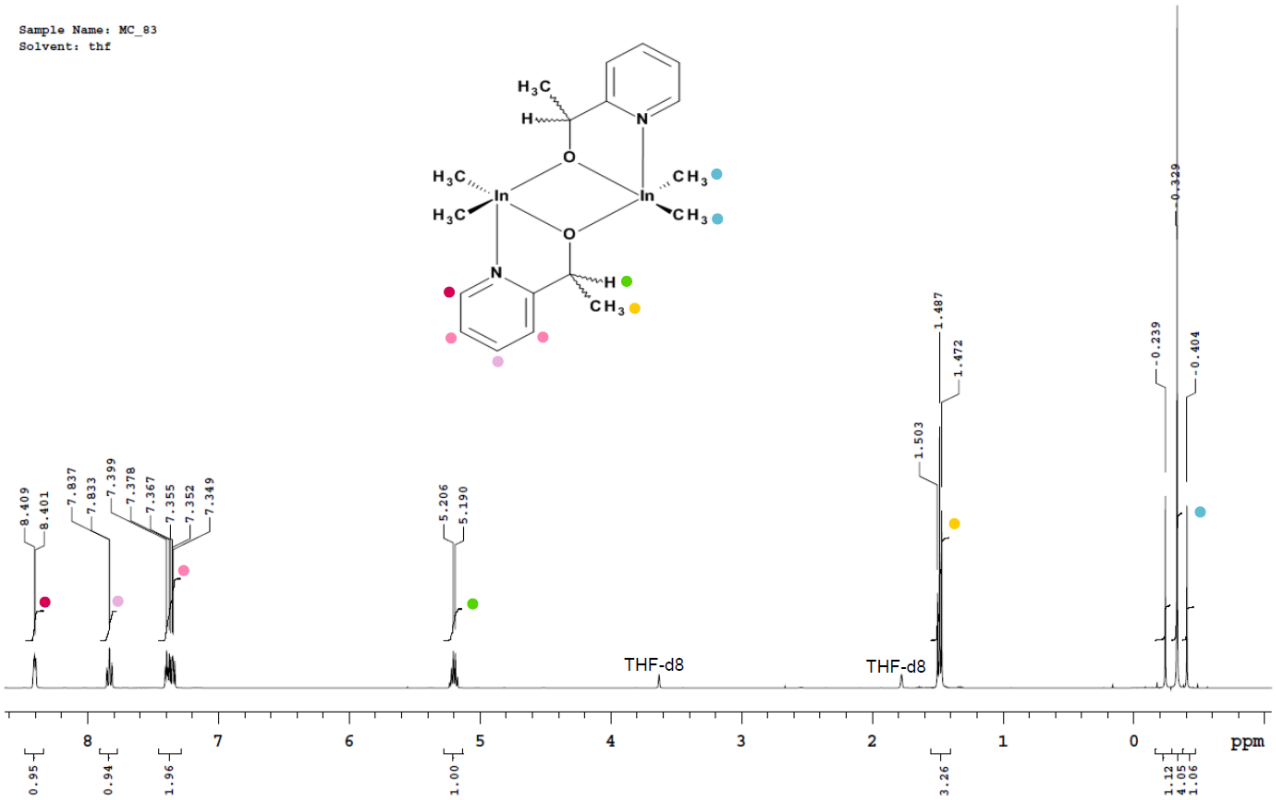

Figure S33. ^{1}H NMR (THF-d_8, 400 MHz) spectrum of **4**.

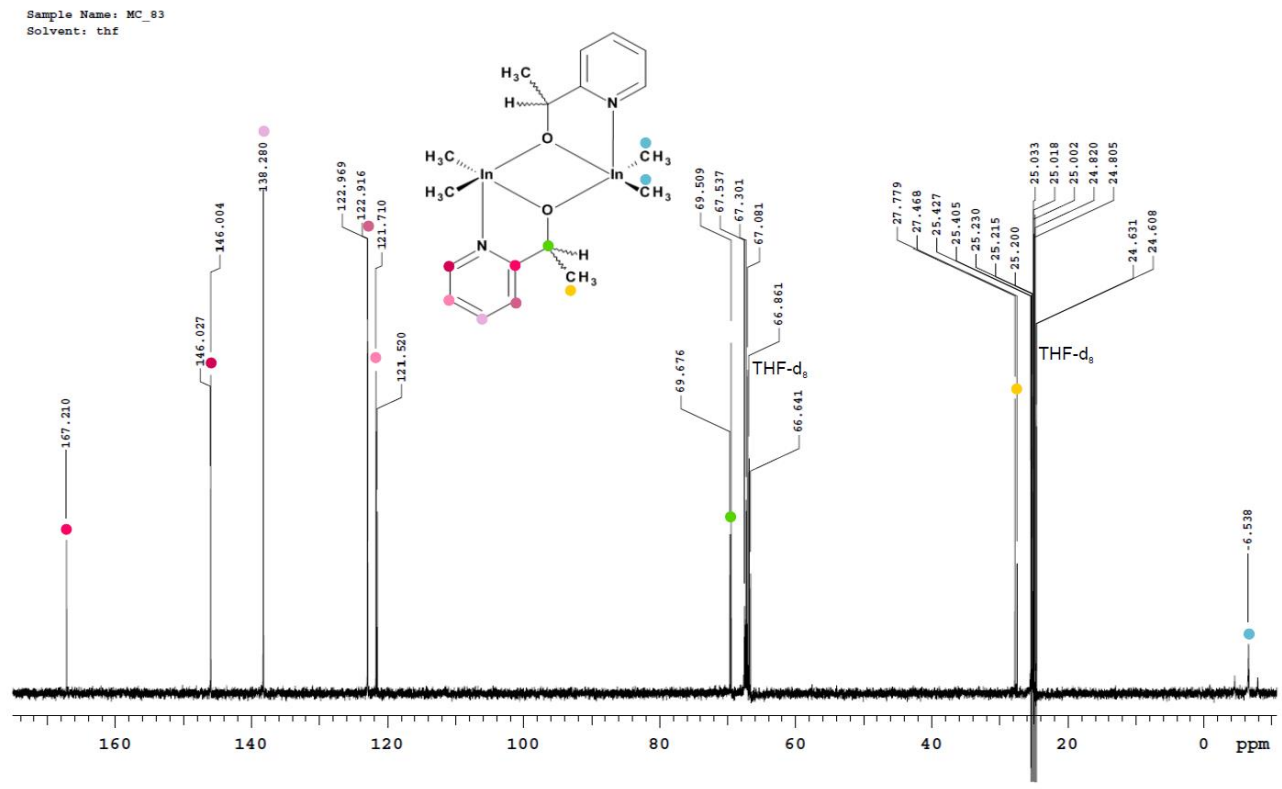

Figure S34. ^{13}C NMR (THF-d_8, 100 MHz) spectrum of **4**.

2) DOSY NMR - Pulsed Field-Gradient Spin Echo NMR (PGSE NMR)

All PGSE NMR experiments were performed on Agilent 600 MHz spectrometer (Agilent, USA) equipped with the Penta probe at temperature set to 25 °C. The measurements were acquired using Gradient Compensated Stimulated Echo sequence (Diffusion delay was set to 50 ms, and the diffusion gradient length to 2ms) using 32 logarithmically sampled pulse-field gradients with strength varying between 2 Gs/cm to 40 Gs/cm. Each FID was acquired with 8 scans on 16384 complex points.

The data was first Fourier transformed and zero-filling and exponential weighting function, set to 2Hz, were applied. Each peak was integrated and integral values were used as an input for Iterative Thresholding Algorithm for Multiexponential Decay (ITAMeD)[1] (1e4 iterations τ set to 1e-5). The diffusion coefficient for each peak was determined as the center of the peak from diffusion coefficient distribution provided by ITAMeD.

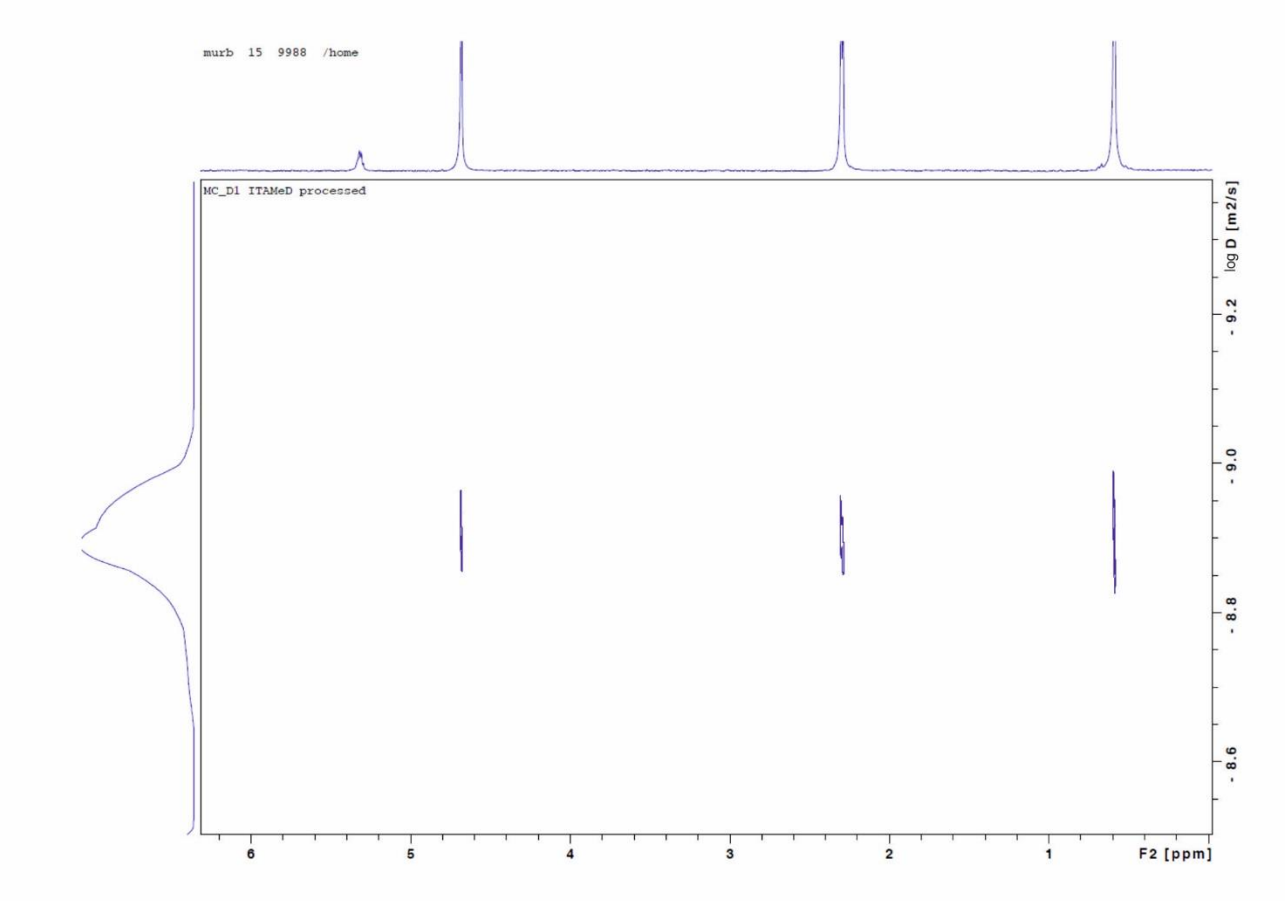

Figure S35. DOSY NMR spectrum of (*S*,*S*)-**1** (CD_2Cl_2, 600MHz, 25ºC).

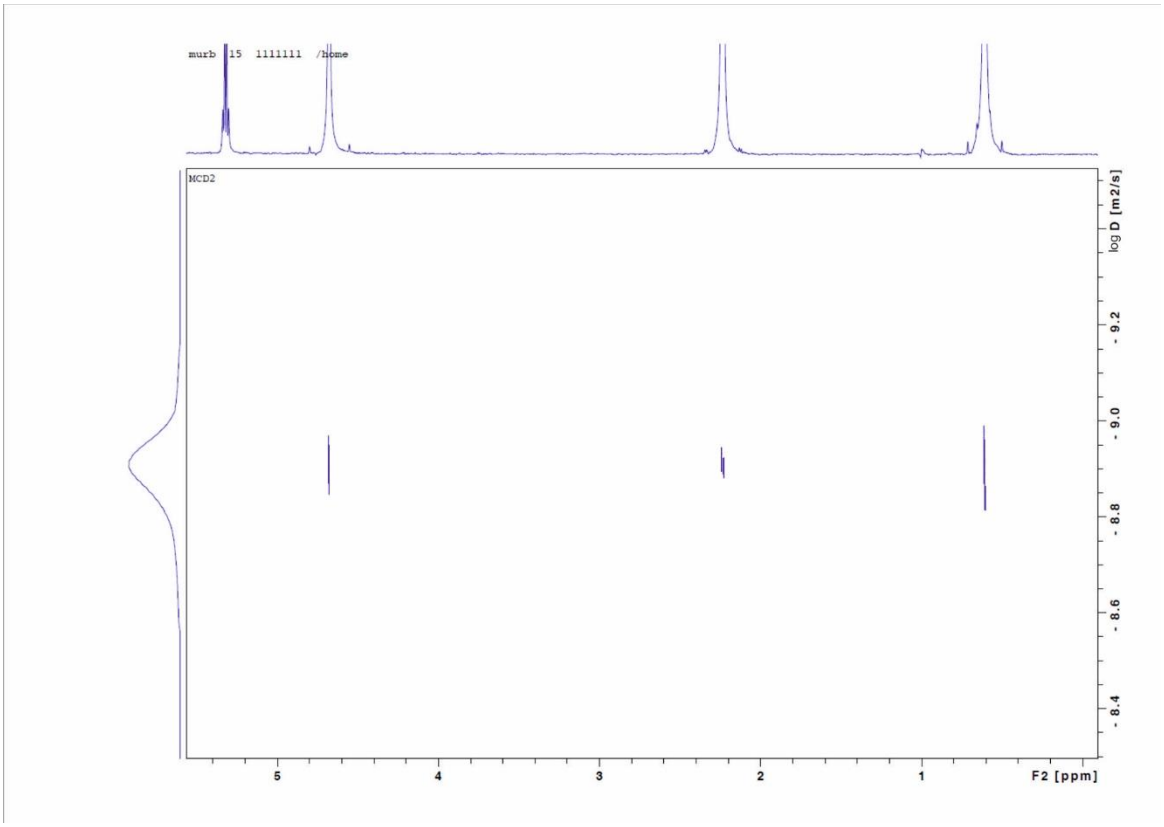

Figure S36. DOSY NMR spectrum of (*S*,*S*)-**2** (CD_2Cl_2, 600MHz, 25ºC).

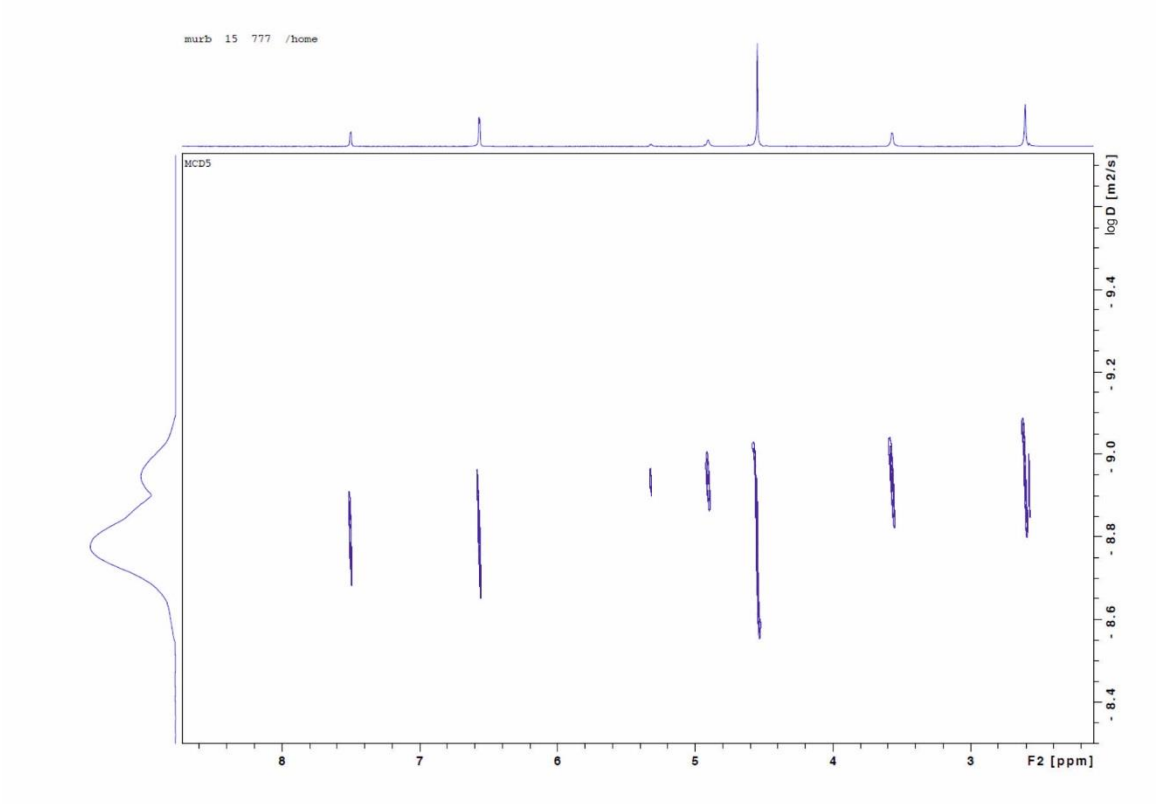

Figure S37. DOSY NMR spectrum of (*S*,*S*)-**1**/DMAP (1:6) (CD_2Cl_2, 600MHz, 25ºC).

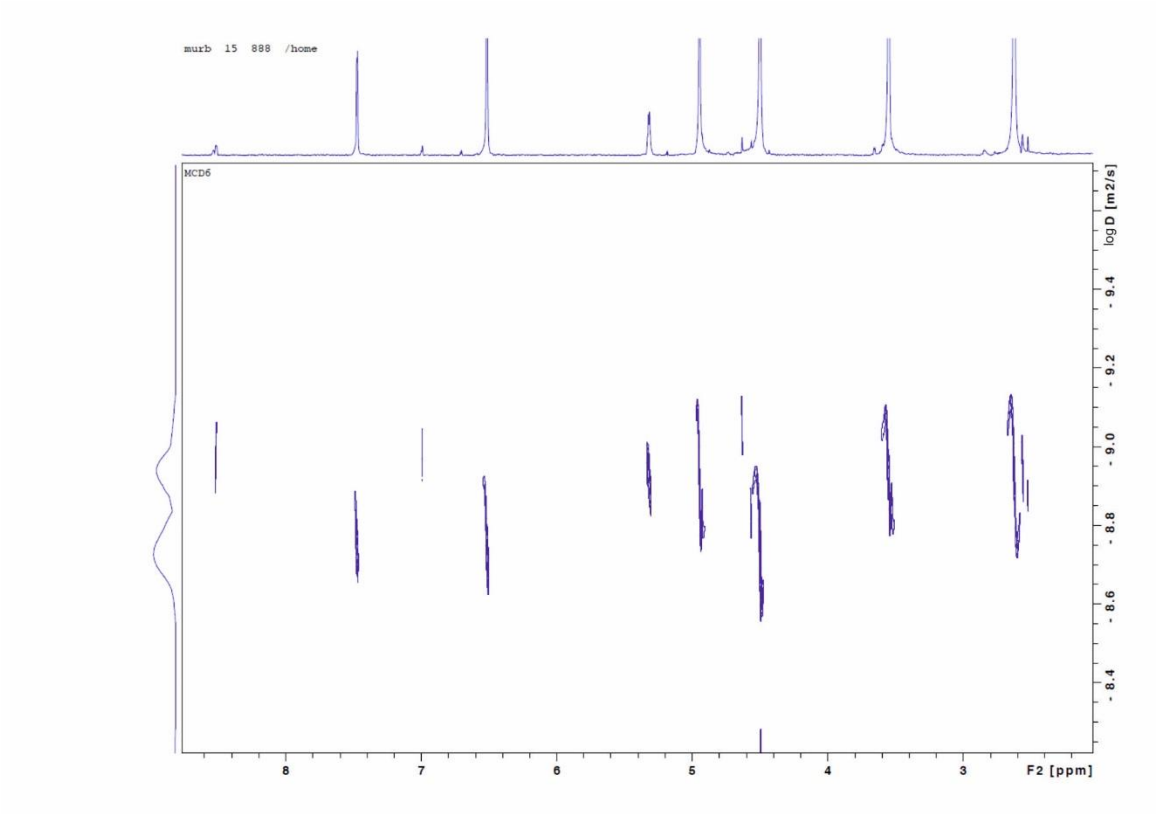

Figure S38. DOSY NMR spectrum of (*S*,*S*)-**2**/DMAP (1:6) (CD_2Cl_2, 600MHz, 25ºC).

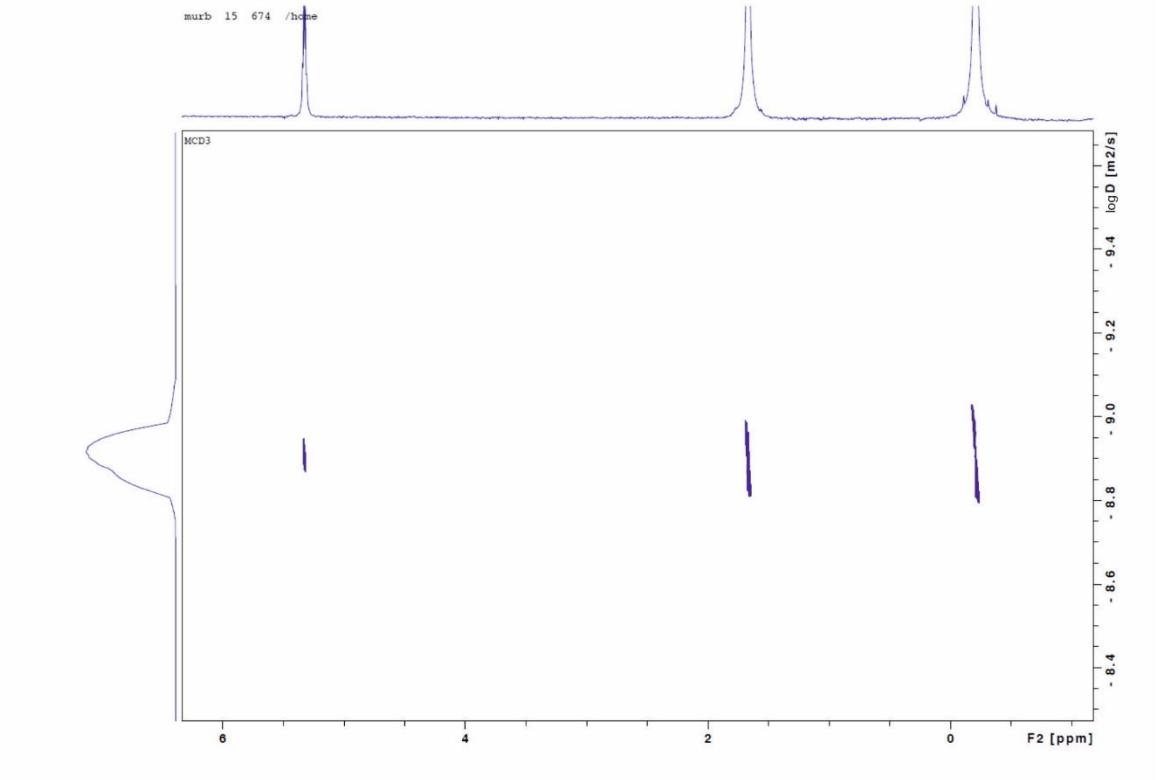

Figure S39. DOSY NMR spectrum of **3** (CD_2Cl_2, 600MHz, 25ºC).

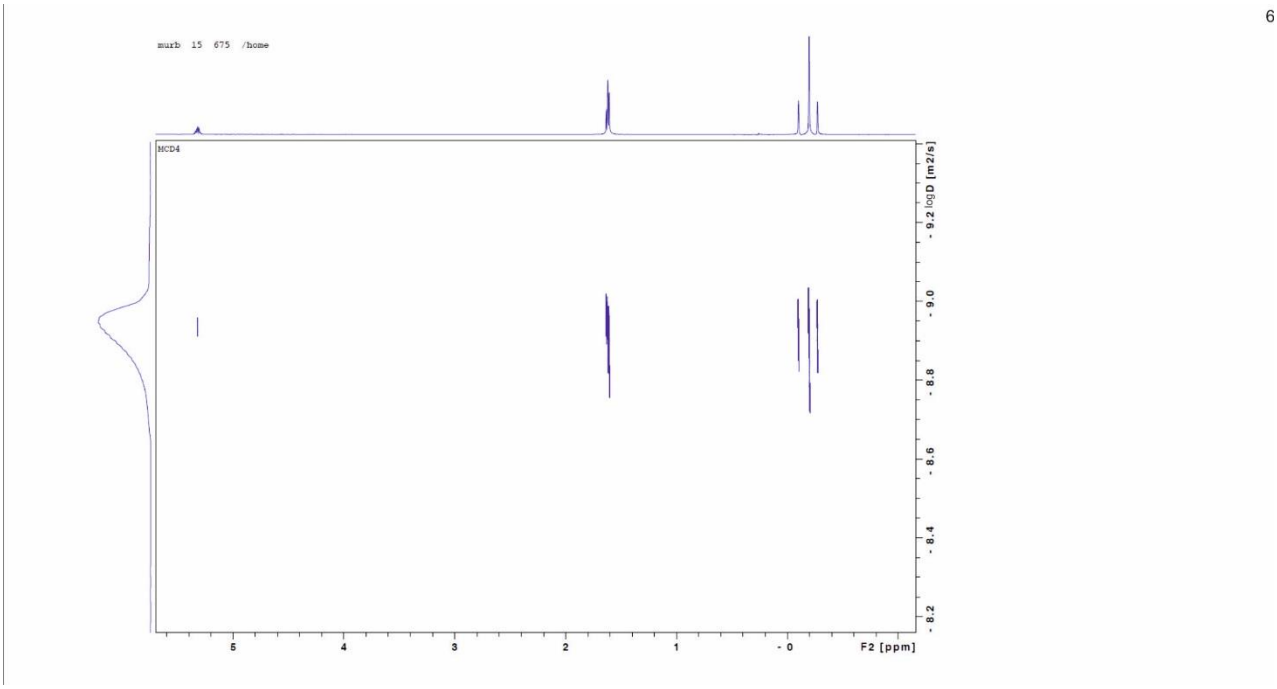

Figure S40. DOSY NMR spectrum of **4** (CD_2Cl_2, 600MHz, 25ºC).

3) FTIR

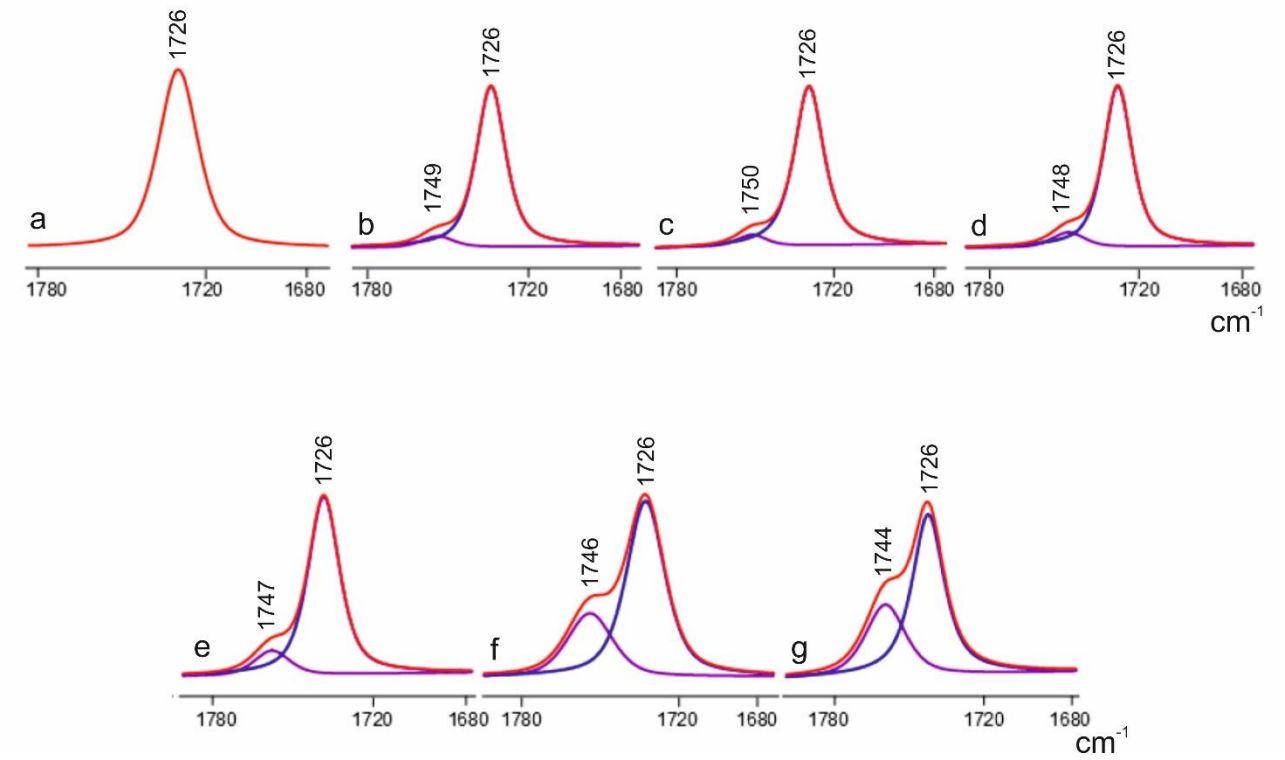

Figure S41. FTIR spectra in the region of C=O band of (*S*,*S*)-**1** (1% in toluene) (a), (*S*,*S*)-**1**/TEA (1:6) (b), (*S*,*S*)-**1**/2,4,6-trimethylpyridine (1:6) (c), (*S*,*S*)-**1**/DMEA (1:6) (d), (*S*,*S*)-**1**/pyridine (1:6) (e), (*S*,*S*)-**1**/ γ-picoline (1:6) (f), (*S*,*S*)-**1**/DMAP (1:6) (g). The original band is indicated in red. Purple and blue bands represent bands of free and coordinated C=O groups, respectively, obtained after deconvolution. Shifts correspond to bands obtained after deconvolution process.

Table S1. The percentage of free C=O groups for (*S*,*S*)-**1**/6equiv. of amine (in toluene) calculated on the basis of FTIR spectra presented on Figure S41.

System	Free C=O (%)
(*S*,*S*)-**1**	0
(*S*,*S*)-**1**/TEA (1:6)	6
(*S*,*S*)-**1**/2,4,6-trimethylpyridine (1:6)	6
(*S*,*S*)-**1**/DMEA (1:6)	9
(*S*,*S*)-**1**/pyridine (1:6)	11
(*S*,*S*)-**1**/γ-picoline (1:6)	28
(*S*,*S*)-**1**/DMAP (1:6)	34

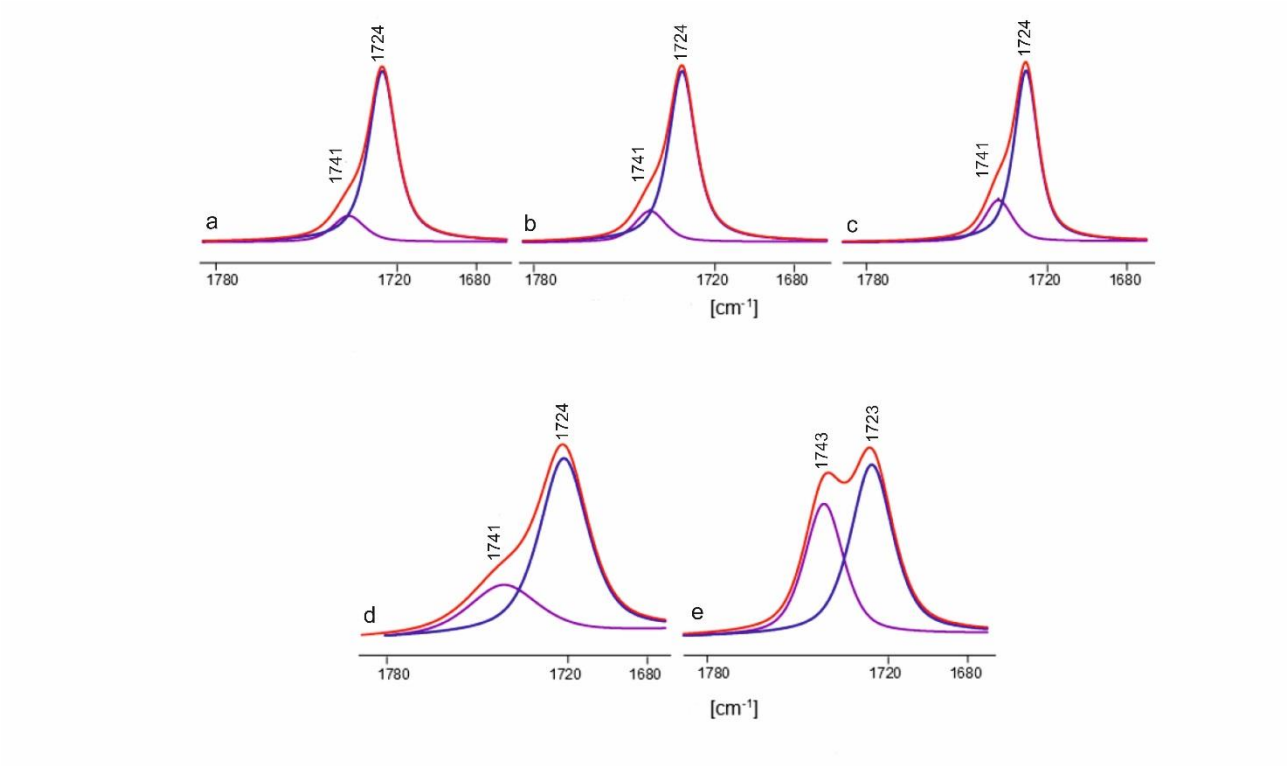

Figure S42. FTIR spectra in the region of C=O band (1% in CH_2Cl_2) of (*S*,*S*)-**1**/pyridine (1:1) (a), (*S*,*S*)-**1**/pyridine (1:2) (b), (*S*,*S*)-**1**/pyridine (1:6) (c), (*S*,*S*)-**1**/pyridine (1:60) (d), (*S*,*S*)-**1** in pyridine (e). The original band is indicated in red. Purple and blue bands represent bands of free and coordinated C=O groups, respectively, obtained after deconvolution. Shifts correspond to bands obtained after deconvolution process.

Table S2. The percentage of free C=O groups for (*S*,*S*)-**1**/6equiv. of amine (in CH_2Cl_2) calculated on the basis of FTIR spectra presented on Figure S42.

System	Free C=O (%)
(*S*,*S*)-**1**/pyridine (1:1)	14
(*S*,*S*)-**1**/pyridine (1:2)	16
(*S*,*S*)-**1**/pyridine (1:6)	21
(*S*,*S*)-**1**/pyridine (1:60)	28
(*S*,*S*)-**1** in pyridine	41

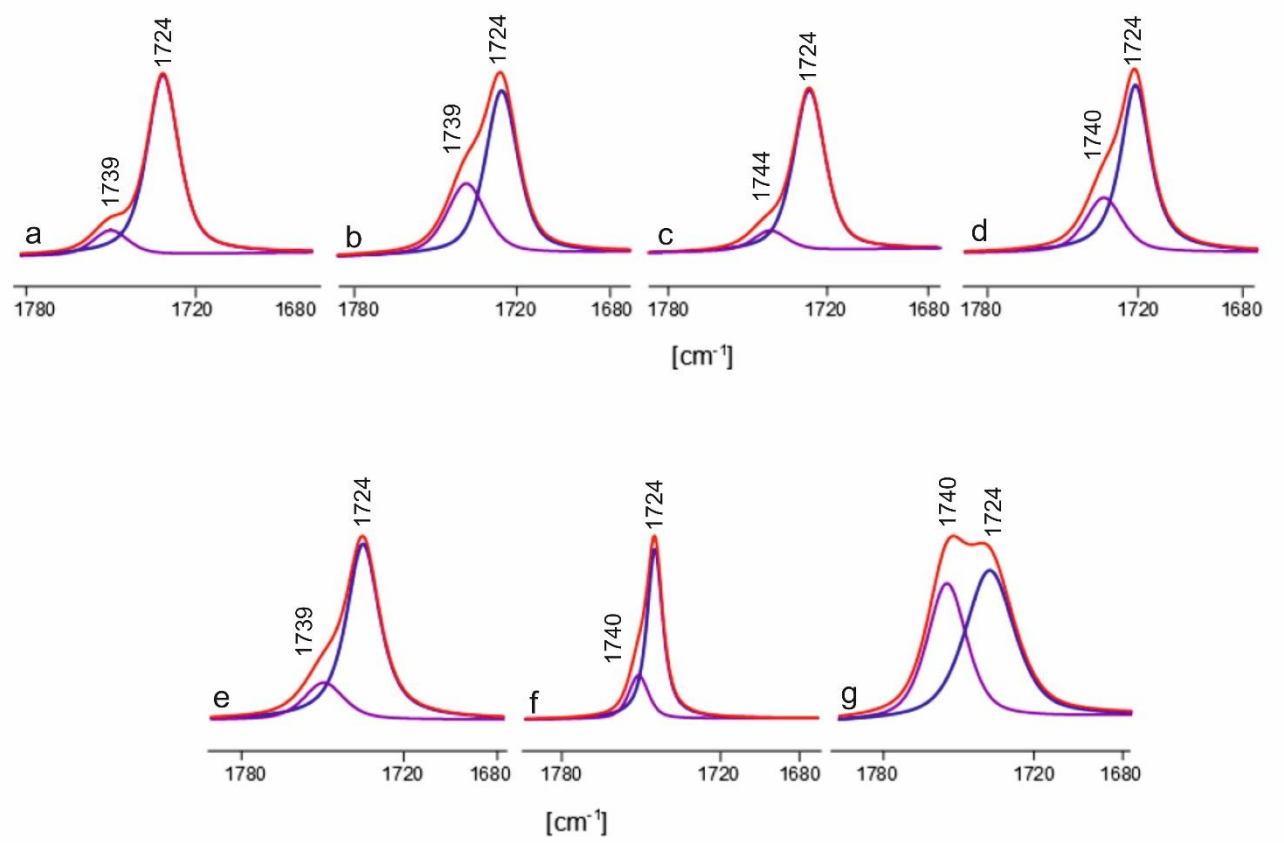

Figure S43. FTIR spectra in the region of C=O band of (*S*,*S*)-**1** (1% in CH_2Cl_2) (a), (*S*,*S*)-**1**/TEA (1:6) (trimethylamine) (b), (*S*,*S*)-**1**/2,4,6-trimethylpyridine (1:6) (c), (*S*,*S*)-**1**/DMEA (1:6) (d), (*S*,*S*)-**1**/pyridine (1:6) (e), (*S*,*S*)-**1**/γ-picoline (1:6) (f), (*S*,*S*)-**1**/DMAP (1:6) (g). The original band is indicated in red. Purple and blue bands represent bands of free and coordinated C=O groups, respectively, obtained after deconvolution. Shifts correspond to bands obtained after deconvolution process.

Table S3. The percentage of free C=O groups for (*S*,*S*)-**1**/amine (1:6) (in CH_2Cl_2) calculated on the basis of FTIR spectra presented on Figure S43.

System	Free C=O (%)
(*S*,*S*)-**1**	12
(*S*,*S*)-**1**/6equiv. TEA	22
(*S*,*S*)-**1**/6equiv. 2,4,6-trimethylpyridine	12
(*S*,*S*)-**1**/6equiv. DMEA	25
(*S*,*S*)-**1**/6equiv. pyridine	21
(*S*,*S*)-**1**/6equiv. γ-picoline	34
(*S*,*S*)-**1**/6equiv. DMAP	42

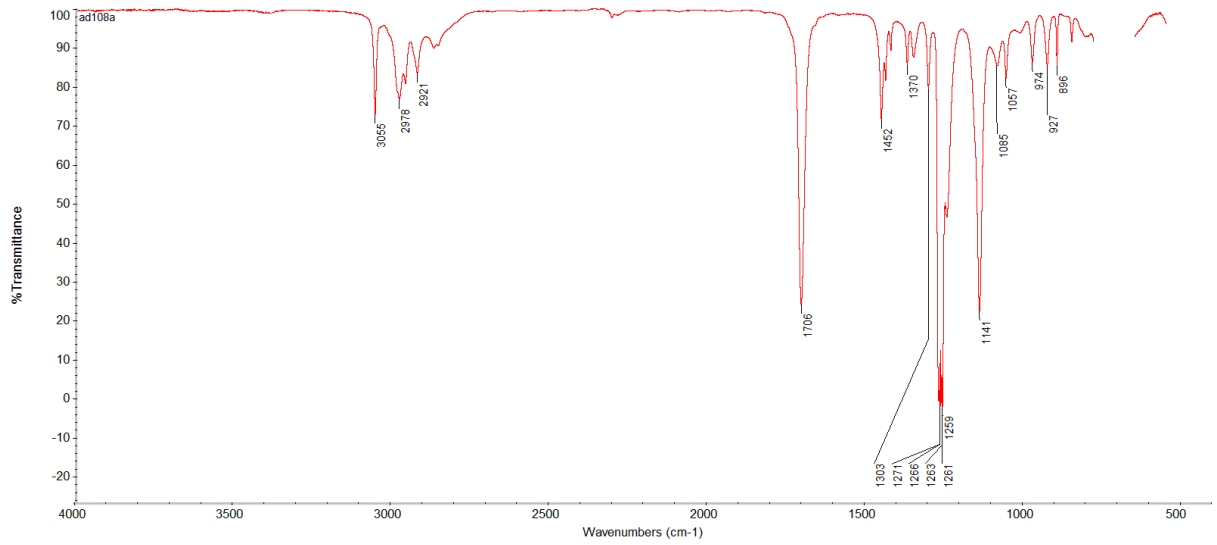

Figure S44. FTIR spectra of (*S*,*S*)-**2** (1% in CH_2Cl_2)

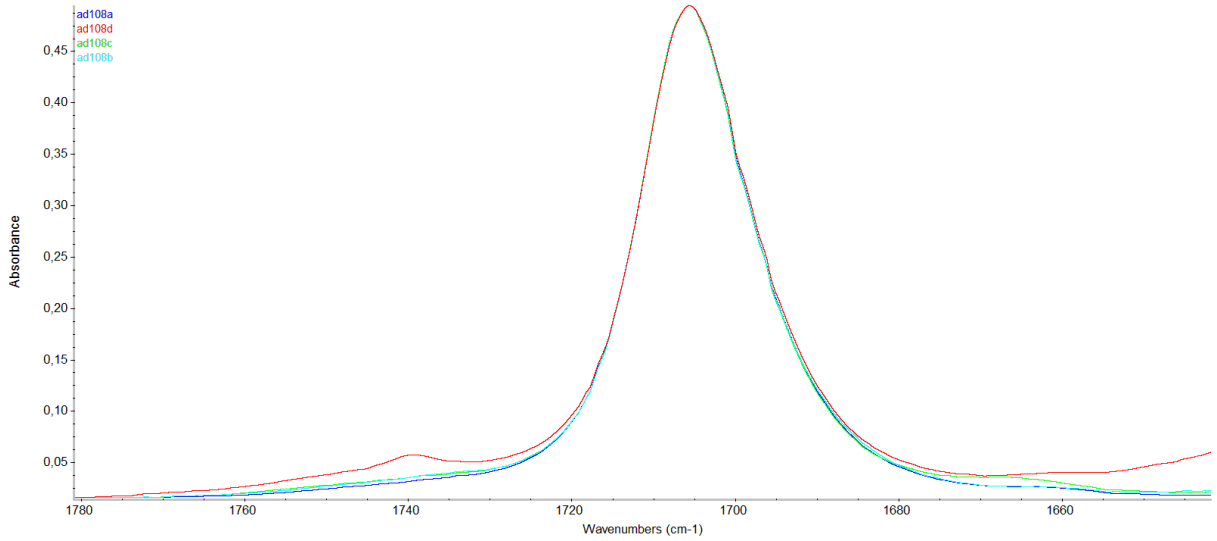

Figure S45. FTIR spectra in the region of C=O band (1% in CH_2Cl_2) of, (*S*,*S*)-**2** (ad108a), (*S*,*S*)-**2**/pyridine (1:6) (ad108b), (*S*,*S*)-**2**/γ-picoline (1:6) (ad108c), (*S*,*S*)-**2**/DMAP (1:6) (ad108d).

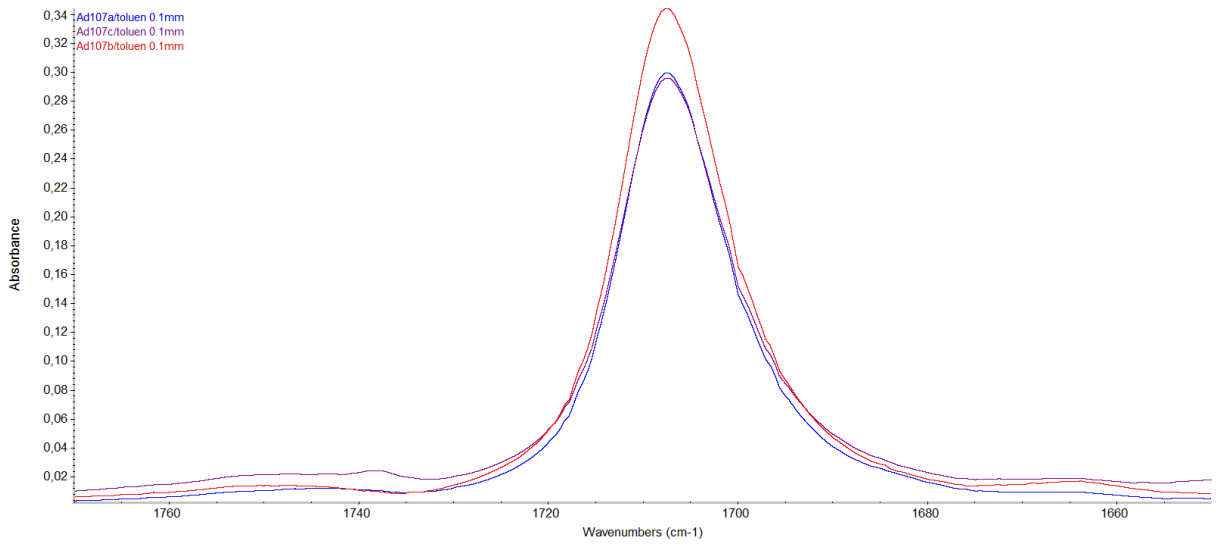

Figure S46. FTIR spectra in the region of C=O band (1% in toluene) of, (*S*,*S*)-**2** with 6equiv. of pyridine (a), (*S*,*S*)-**2** with 6equiv. of γ-picoline (b), (*S*,*S*)-**2** with 6equiv. of DMAP (c).

4) Polymerization data

Table S4. Polymerization of *rac*-LA with (*S*,*S*)-**1**/amine 40ºC with LA/Ga = 50:1.

No.	Cat.	t [h]	Conv. [%]	10^{-3} M_n[c]	10^{-3} M_n[d]	10^{-3} M_n[e]	M_w/M_n	P_r[f]	P_r[g]
1[a]	(*S*,*S*)-**1**	96	58	6.7	3.2	4.3	1.02	0.49	-
2[a]	(*S*,*S*)-**1**/Et_3N (1:6)	96	63	7.2	3.7	4.6	1.01	0.50	-
3[a]	(*S*,*S*)-**1**/2,4,6-colidine (1:6)	96	52	7.4	3.1	3.9	1.01	0.50	-
4[a]	(*S*,*S*)-**1**/Me_2NEt (1:6)	96	68	6.2	3.6	5.0	1.01	0.50	0.50
5[a]	(*S*,*S*)-**1**/pyridine (1:1)	96	64	7.4	3.8	4.7	1.01	0.51	0.51
6[a]	(*S*,*S*)-**1**/pyridine (1:2)	96	69	7.0	4.2	5.1	1.02	0.56	0.56
7[a]	(*S*,*S*)-**1**/pyridine (1:6)	96	90	8.2	6.8	6.6	1.03	0.69	0.68
8[a]	(*S*,*S*)-**1**/pyridine (1:60)	96	96	8.3	7.5	7.0	1.15	0.77	0.77
9[a]	(*S*,*S*)-**1** (in pyridine)	96	90	6.7	5.9	6.6	1.04	0.66	0.65
10[a]	(*S*,*S*)-**1**/γ-picoline (1:6)	96	94	7.9	7.2	6.9	1.02	0.75	0.74
11[a]	(*S*,*S*)-**1**/DMAP (1:6)	96	90	7.5	6.4	6.6	1.05	0.85	0.86
12[a]	(*S*,*S*)-**1**/DMAP (1:60)	96	64	-	2.9	4.7	-	0.70	-
13[b]	(*S*,*S*)-**1**	96	87	7.2	6.5	6.4	1.01	0.50	-
14[b]	(*S*,*S*)-**1**/Et_3N (1:6)	24	33	-	1.5	2.5	-	-	-
15[b]	(*S*,*S*)-**1**/Et_3N (1:6)	96	72	7.4	5.1	5.3	1.01	0.55	-
16[b]	(*S*,*S*)-**1**/2,4,6-colidine (1:6)	96	82	6.6	5.1	6.0	1.01	0.50	-
17[b]	(*S*,*S*)-**1**/Me_2NEt (1:6)	24	59	-	3.5	4.3	-	-	-

18[b]	(*S*,*S*)-**1**/Me_2NEt (1:6)	96	93	7.5	6.9	6.8	1.03	0.70	-
19[b]	(*S*,*S*)-**1**/pyridine (1:6)	24	48	-	1.9	3.5	-	-	-
20[b]	(*S*,*S*)-**1**/pyridine (1:6)	96	79	6.8	4.9	7.0	1.01	0.65	-
21[b]	(*S*,*S*)-**1**/γ-picoline (1:6)	24	65	-	3.8	4.8	-	-	-
22[b]	(*S*,*S*)-**1**/γ-picoline (1:6)	96	92	8.1	7.4	6.7	1.03	0.71	-
23[b]	(*S*,*S*)-**1**/γ-picoline (1:60)	24	0.76	-	5.4	5.6	-	-	-
24[b]	(*S*,*S*)-**1**/γ-picoline (1:60)	96	0.88	-	7.2	6.4	-	-	-
25[b]	(*S*,*S*)-**1**/DMAP (1:6)	24	75	-	4.5	5.5	-	-	-
26[b]	(*S*,*S*)-**1**/DMAP (1:6)	96	96	6.5	7.1	7.0	1.07	0.63	-

[a] in toluene. [b] in CH_2Cl_2. [c] Determined by gel permeation chromatography (GPC) in THF. [d] Determined by ^{1}H NMR; [e] expected value calculated according to LA/Ga ratio and conversion. [f] calculated on the basis of homonuclear decoupled ^{1}H NMR spectra according to Chamberlain et al.[2] [g] Calculated on the basis of ^{13}C NMR[3]

Table S5. Polymerization of *rac*-LA with **3**/amine at 40ºC and r.t with LA/In = 50:1.

No.	Cat.	t [h]	Conv. [%]	10^{-3} M_n[c]	10^{-3} M_n[d]	10^{-3} M_n[e]	M_w/M_n	P_r[f]	P_r[g]
1[a]	(*S*,*S*)-**2**	24	88	3.4	3.4	3.3	1.17	0.55	-
2[a]	(*S*,*S*)-**2**/2,4,6-colidine (1:6)	24	94	8.2	6.5	6.9	1.03	0.55	0.54
3[a]	(*S*,*S*)-**2**/Et_3N (1:6)	120	>99	9.6	7.5	7.3	1.06	0.54	0.54
4[a]	(*S*,*S*)-**2** /Me_2NEt (1:6)	24	96	8.3	7.5	7.0	1.08	0.65	0.66
5[a]	(*S*,*S*)-**2** /pyridine (1:2)	24	99	7.6	7.8	7.2	1.12	0.67	0.69
6[a]	(*S*,*S*)-**2** /pyridine (1:6)	24	98	8.4	7.4	7.2	1.20	0.69	0.69

7[a]	(*S*,*S*)-**2** /pyridine (1:60)	24	99	5.0	6.9	7.2	1.98	0.68	0.69
8[a]	(*S*,*S*)-**2**/γ-picoline (1:6)	24	99	6.2	7.1	7.2	1.53	0.65	0.66
9[a, i]	(*S*,*S*)-**2**/DMAP (1:6)	24	>99	1.7	4.0	3.7	2.32	0.49	-
10[a,h]	(*S*,*S*)-**2**	216	83	-	5.5	6.1	-	0.58	0.58
11[a,h]	(*S*,*S*)-**2** /pyridine (1:2)	144	98	-	6.3	7.2	-	0.67	0.67
12[a,h]	(*S*,*S*)-**2** /pyridine (1:6)	48	97	-	6.1	7.1	-	0.71	0.71
13[a,h]	(*S*,*S*)-**2** /pyridine (1:60)	24	98	-	7.5	7.2	-	0.72	0.72
14[a,h]	(*S*,*S*)-**2**/γ-picoline (1:6)	24	76	-	4.4	5.5	-	0.65	0.64
15[a,h]	(*S*,*S*)-**2**/DMAP (1:6)	24	>99	2.7	5.6	7.3	3.27	0.53	-
16[b]	(*S*,*S*)-**2**	24	84	7.3	4.9	6.1	1.04	0.50	-
17[b]	(*S*,*S*)-**2**/2,4,6-colidine (1:6)	24	82	7.1	5.3	6.0	1.06	0.49	-
18[b]	(*S*,*S*)-**2**/Et_3N (1:6)	24	90	7.8	6.4	6.7	1.11	0.54	-
19[b]	(*S*,*S*)-**2** /Me_2NEt (1:6)	24	99	4.3	6.4	7.2	2.02	0.52	-
20[b,i]	(*S*,*S*)-**2** /pyridine (1:6)	24	>99	3.9	3.7	3.7	1.29	0.66	-
21[b]	(*S*,*S*)-**2**/γ-picoline (1:6)	24	>99	7.1	5.9	7.0	1.13	0.61	-
22[b]	(*S*,*S*)-**2**/DMAP (1:6)	24	96	2.7	5.5	7.0	2.31	0.49	-

[a] in toluene. [b] in CH_2Cl_2. [c] Determined by gel permeation chromatography (GPC) in THF. [d] Determined by ^1H NMR; [e] Calculated according to LA/Ga ratio and conversion. [f] calculated on the basis of homonuclear decoupled ^1H NMR spectra according to Chamberlain et al.[2] [g] Calculated on the basis of ^{13}C NMR.[3] [h] at room temperature, [i] with LA/Ga ratio = 25:1.

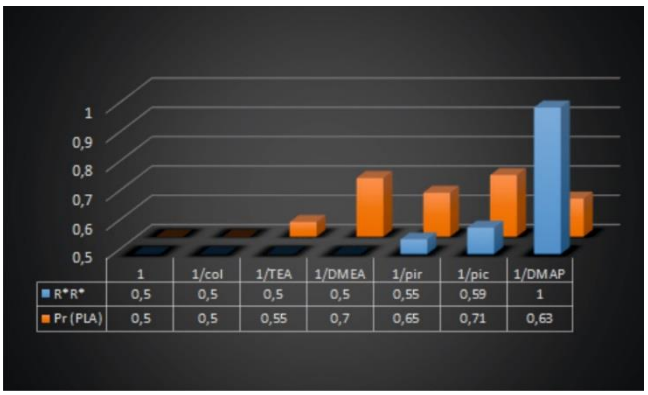

Figure S47. The relation between the excess of homochiral (*R**,*R**)-[$Me_2Ga((\mu$-$OCH(CH_3)CH_2OMe))]_2$ species for **1**/amine, and heteroselectivity of *rac*-LA polymerization with (*S*,*S*)-**1** in CH_2Cl_2 at 40°C. For the polymerization in CH_2Cl_2, the heteroselectivity of [$Me_2Ga((\mu$-$OCH(Me)CH_2OR))]_2$ in the presence of pyridine, γ-picoline and DMAP was lower due to transesterification reactions, however in line with the excess of homochiral species. Surprisingly, the heteroselective polymerization of *rac*-LA in the presence of (*S*,*S*)-**1**/TEA (1:6) (P_r = 0.55) and (*S*,*S*)-**1**/DMEA (1:6) (P_r = 0.70) was observed (see the Supporting Information). Although reactivity of DMEA towards CH_2Cl_2 in the presence of **1** could lead to the formation of new species and slight increase in homochiral species (52%) (see the Supporting Information), the latter result can not be unequivocally explained at this stage but stress once again the need for careful investigation of solvent effect. However, despite slight uncertainity revealed by the nature of active species in CH_2Cl_2, the heteroselectivity of discussed gallium complexes in toluene should be explained by the presence of excess of homochiral dimeric species [$Me_2Ga((\mu$-$OCH(Me)CH_2OR))]_2$ during the polymerization, which was further confirmed by the stereoselectivity of [$Me_2In(\mu$-$OCH(Me)C(O)OR)]_2$.

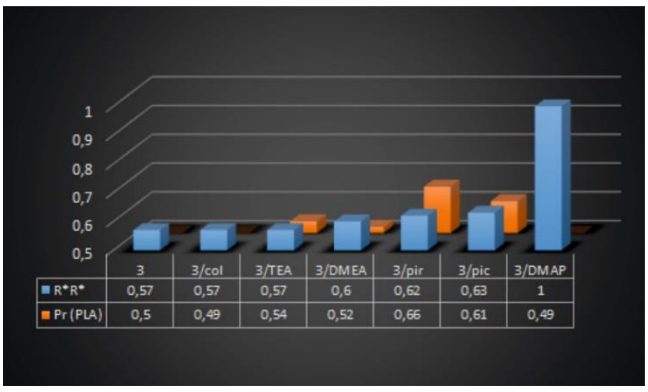

Figure S48. The relation between the excess of homochiral (*R**,*R**)-[$Me_2In((\mu$-$OCH(CH_3)CH_2OMe))]_2$ species for **2**/amine, and heteroselectivity of *rac*-LA polymerization with (*S*,*S*)-**2** in CH_2Cl_2 at 40°C.

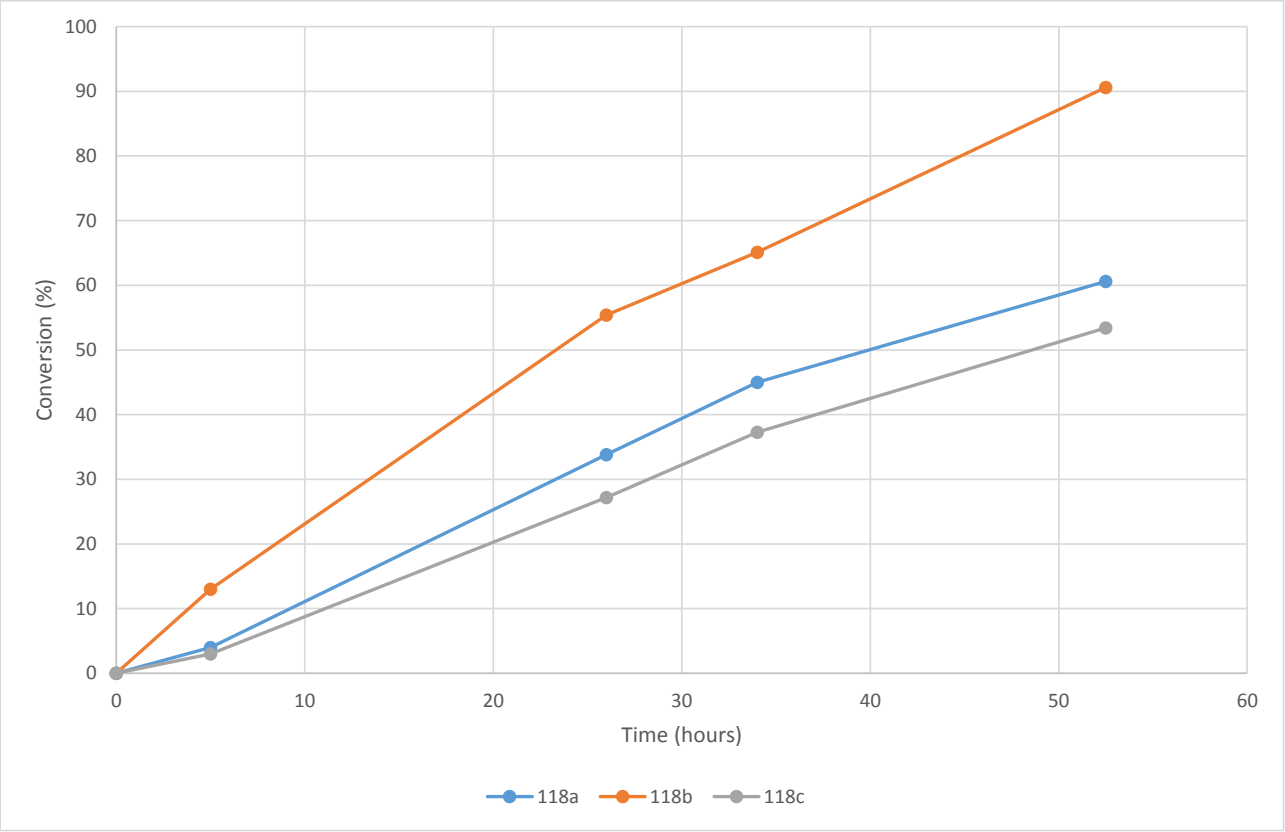

Figure S49. Conversion vs time for the polymerization of *rac*-LA at 40ºC with (*S*,*S*)-**1** (118c), (*S*,*S*)-**1**/pyridine (1:6) (118a), (*S*,*S*)-**1**/DMAP (1:6) (118b).

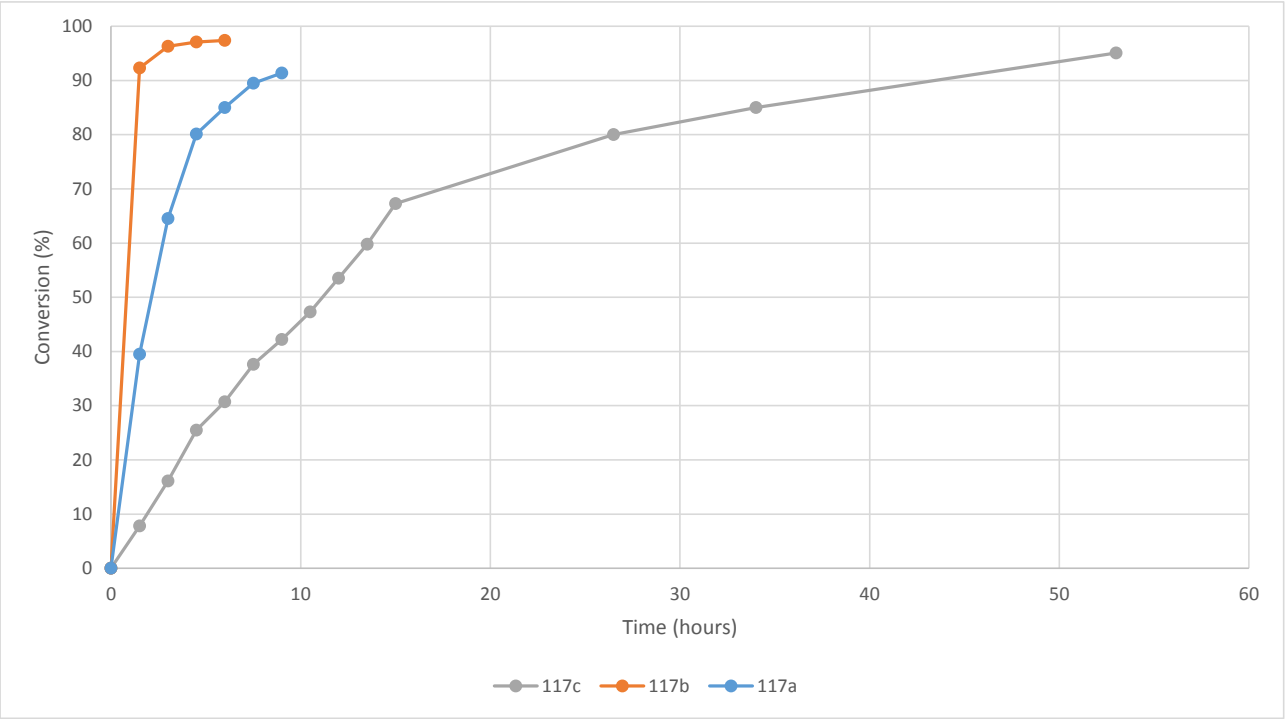

Figure S50. Conversion vs time for the polymerization of *rac*-LA at 40ºC with (*S*,*S*)-**2** (117c), (*S*,*S*)-**2**/pyridine (1:6) (117a), (*S*,*S*)-**2**/DMAP (1:6) (117b).

5) MALDI-TOF

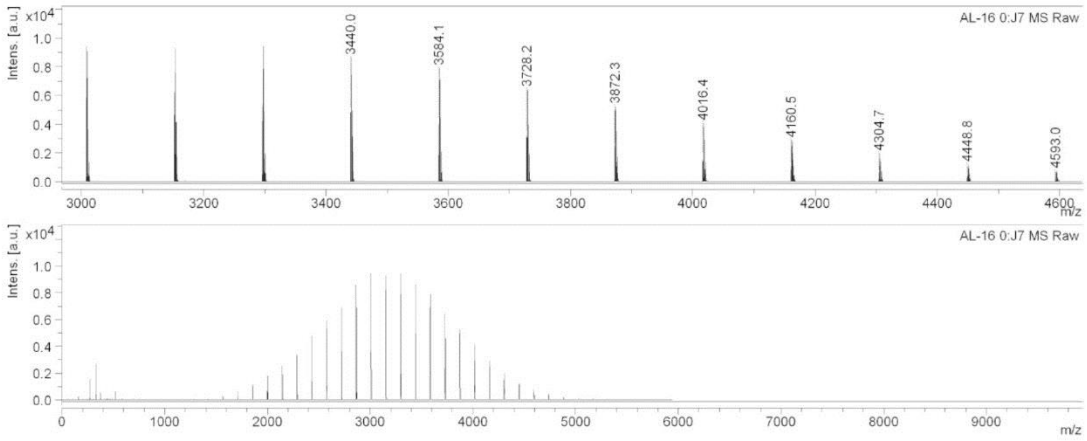

Figure S51. MALDI–TOF spectrum of PLA (T-2-(3-(4-*t*-butyl-phenyl)-2-methyl-2-propenylidene) malononitrile (DCTB) was used as a matrix) obtained by polymerization of 100 equiv. of *rac*-LA with (*S*,*S*)-**1** as initiator, in toluene at 40ºC, 96 h. The distributions refer to PLA with OH and CH(Me)C(O)OMe end groups, with Na^+.

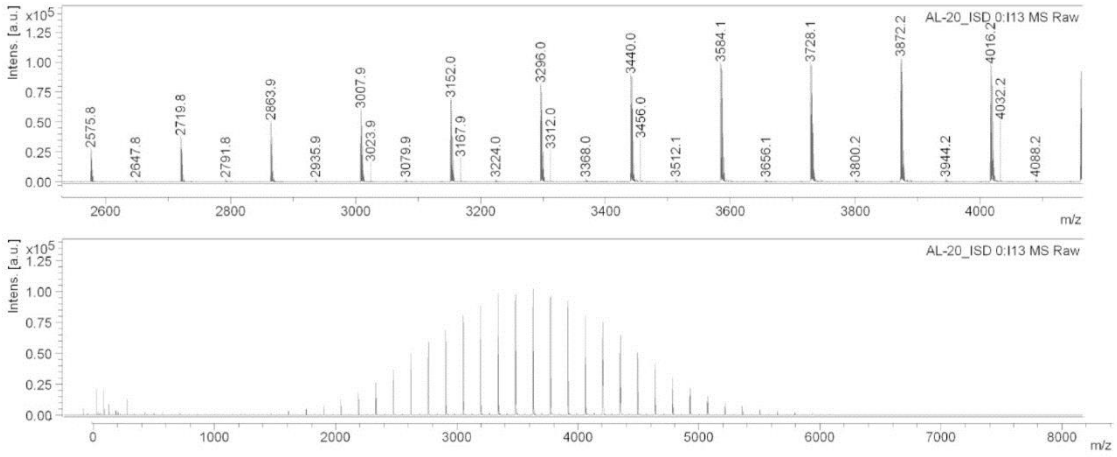

Figure S52. MALDI–TOF spectrum of PLA (T-2-(3-(4-*t*-butyl-phenyl)-2-methyl-2-propenylidene) malononitrile (DCTB) was used as a matrix) obtained by polymerization of 100 equiv. of *rac*-LA with (*S*,*S*)-**1**/DMEA (1:6) as initiator, in toluene at 40ºC, 96 h. The distributions refer to PLA with OH and CH(Me)C(O)OMe end groups, with Na^+.

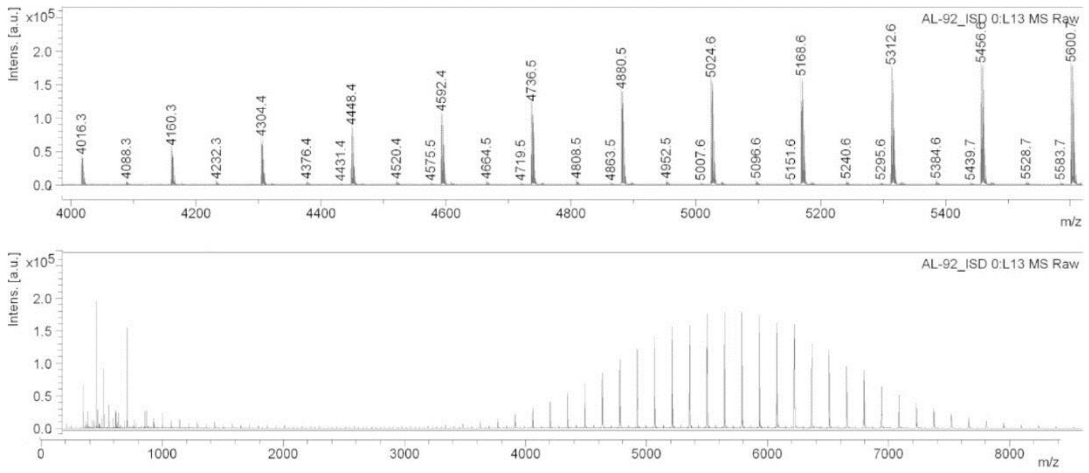

Figure S53. MALDI–TOF spectrum of PLA (T-2-(3-(4-*t*-butyl-phenyl)-2-methyl-2-propenylidene) malononitrile (DCTB) was used as a matrix) obtained by polymerization of 100 equiv. of *rac*-LA with (*S*,*S*)-**1**/ piridine (1:6) as initiator, in toluene at 40ºC, 96 h. The distributions refer to PLA with OH and CH(Me)C(O)OMe end groups, with Na^+.

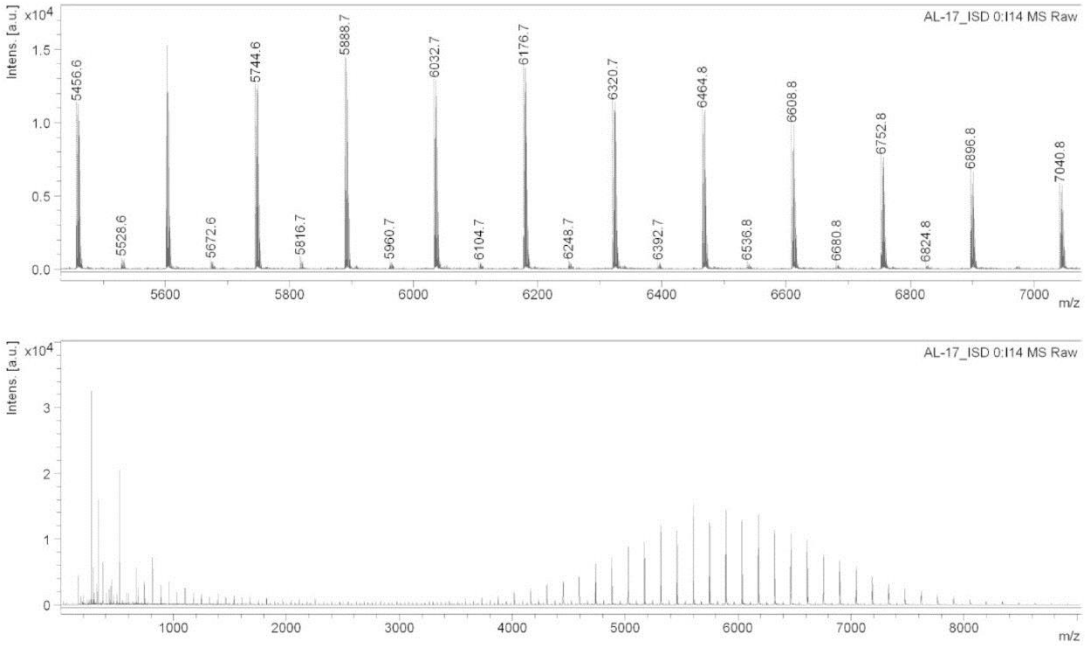

Figure S54. MALDI–TOF spectrum of PLA (T-2-(3-(4-*t*-butyl-phenyl)-2-methyl-2-propenylidene) malononitrile (DCTB) was used as a matrix) obtained by polymerization of 100 equiv. of *rac*-LA with (*S*,*S*)-**1**/ γ-picoline (1:6) as initiator, in toluene at 40ºC, 96 h. The distributions refer to PLA with OH and CH(Me)C(O)OMe end groups, with Na^+.

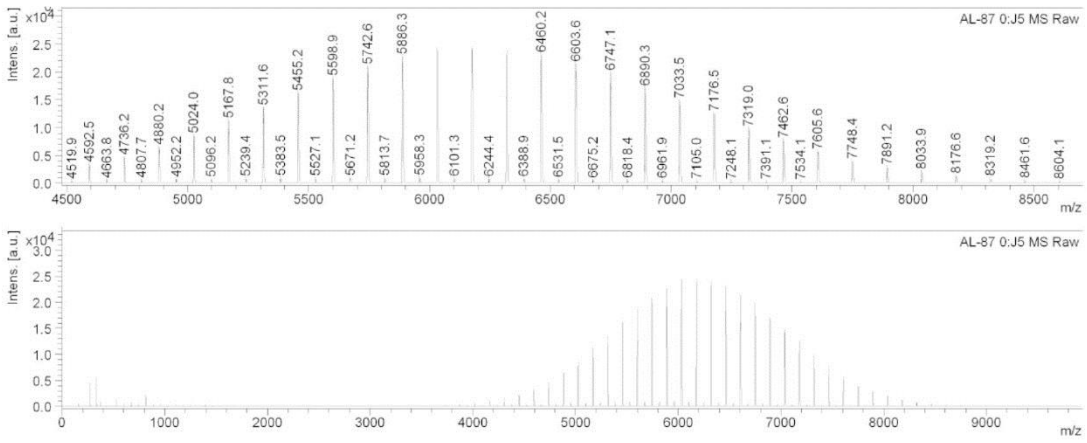

Figure S55. MALDI–TOF spectrum of PLA (T-2-(3-(4-*t*-butyl-phenyl)-2-methyl-2-propenylidene) malononitrile (DCTB) was used as a matrix) obtained by polymerization of 100 equiv. of *rac*-LA with (*S*,*S*)-**1**/ DMAP (1:6) as initiator, in toluene at 40ºC, 96 h. The distributions refer to PLA with OH and CH(Me)C(O)OMe end groups, with Na^+.

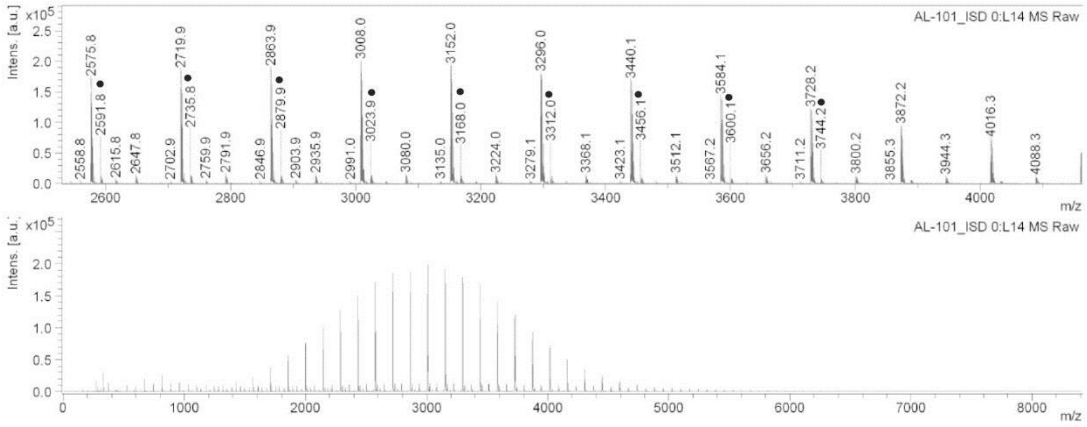

Figure S56. MALDI–TOF spectrum of PLA (T-2-(3-(4-*t*-butyl-phenyl)-2-methyl-2-propenylidene) malononitrile (DCTB) was used as a matrix) obtained by polymerization of 100 equiv. of *rac*-LA with (*S*,*S*)-**1**/ DMAP (1:60) as initiator, in toluene at 40ºC, 96 h. The distributions refer to PLA with OH and CH(Me)C(O)OMe end groups, with Na^+ and K^+ (black dots).

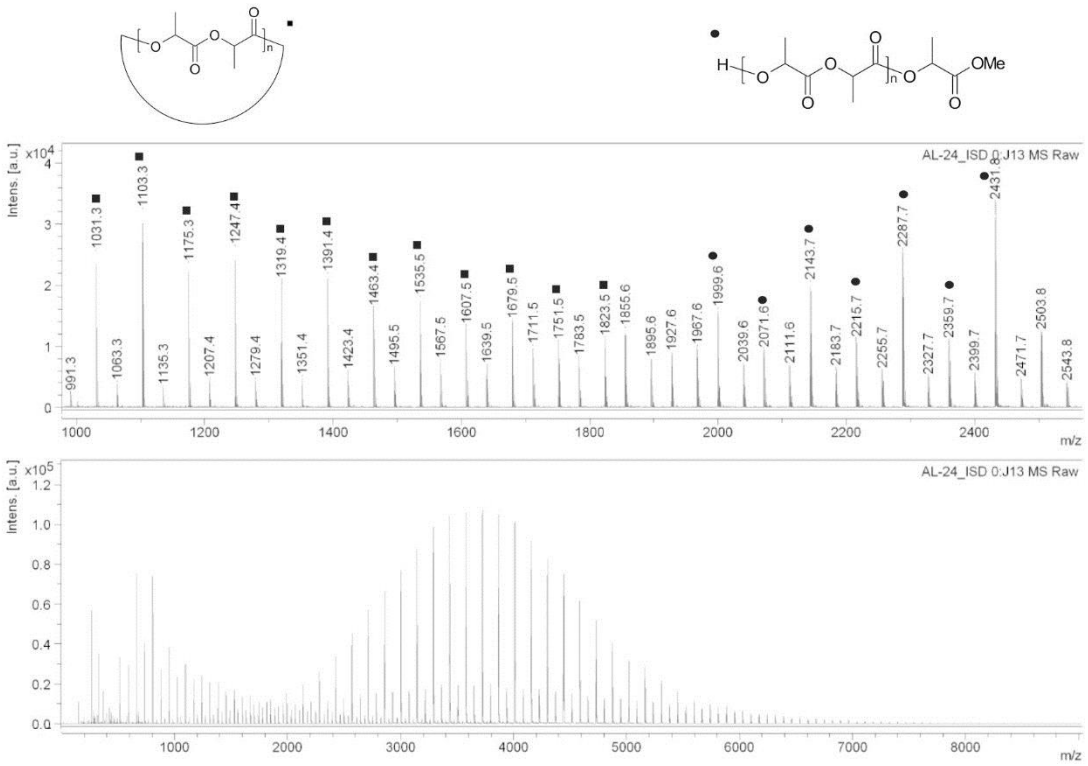

Figure S57. MALDI–TOF spectrum of PLA (T-2-(3-(4-*t*-butyl-phenyl)-2-methyl-2-propenylidene) malononitrile (DCTB) was used as a matrix) obtained by polymerization of 100 equiv. of *rac*-LA with (*S*,*S*)-**1** as initiator, in pyridine at 40ºC, 96 h. The distributions refer to PLA with OH and CH(Me)C(O)OMe end groups and cyclic PLA, with Na^+.

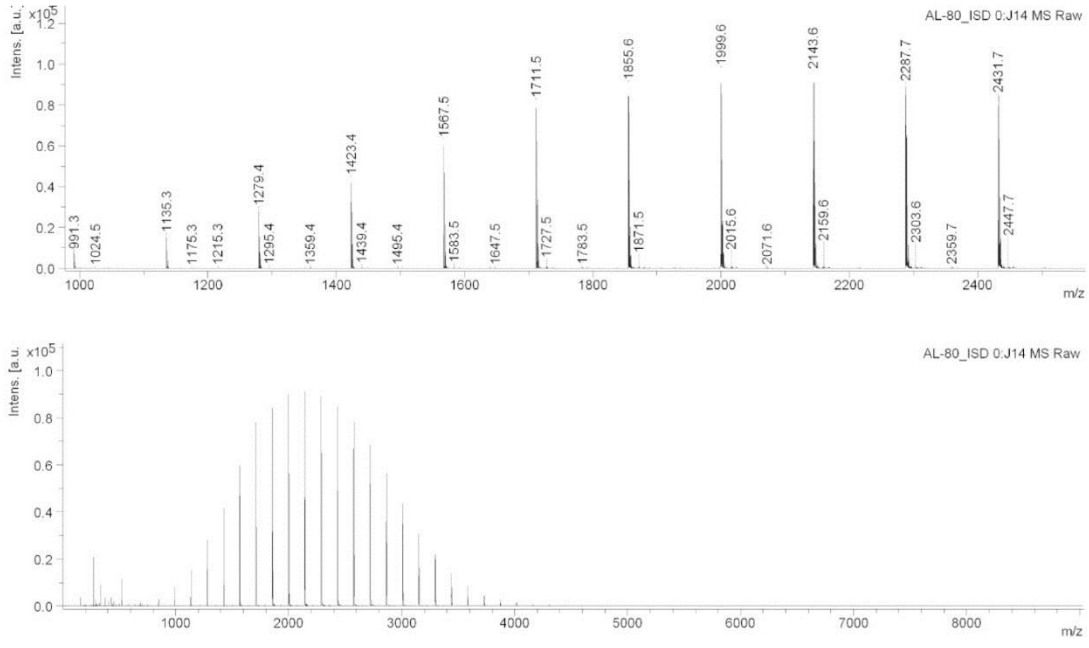

Figure S58. MALDI–TOF spectrum of PLA (T-2-(3-(4-*t*-butyl-phenyl)-2-methyl-2-propenylidene) malononitrile (DCTB) was used as a matrix) obtained by polymerization of 100 equiv. of *rac*-LA with (*S,S*)-**1**/ piridine (1:6) as initiator, in CH_2Cl_2 at 40ºC, 96 h. The distributions refer to PLA with OH and CH(Me)C(O)OMe end groups, with Na^+.

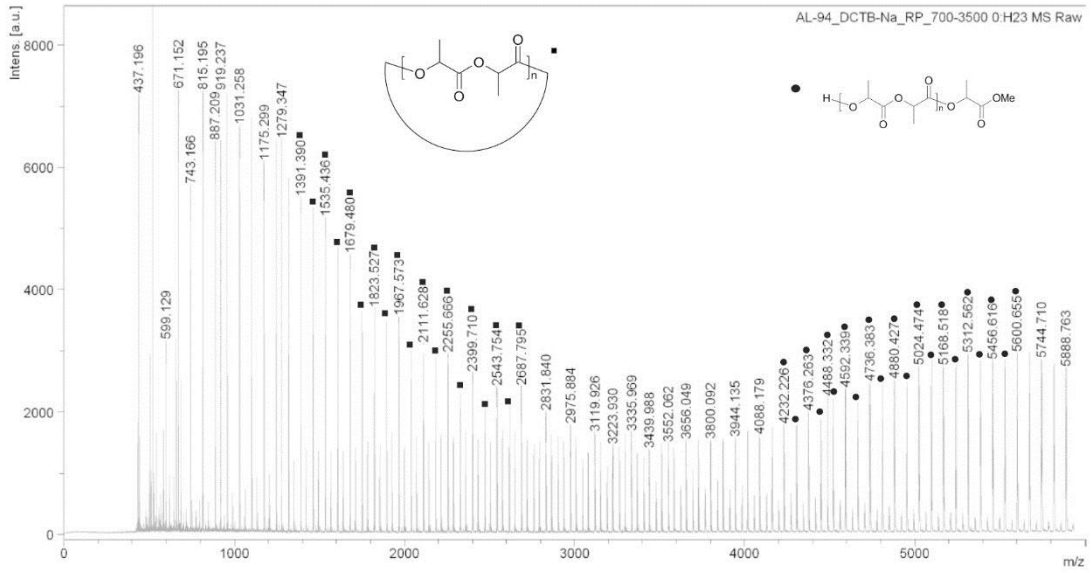

Figure S59. MALDI–TOF spectrum of PLA (2-(4'-Hydroxybenzeneazo)benzoic acid -HABA was used as a matrix) obtained by polymerization of 100 equiv. of *rac*-LA with (*S,S*)-**1**/DMAP as initiator, in CH_2Cl_2 at 40ºC, 24h. The distributions refer to PLA with OH and CH(Me)C(O)OMe end groups and cyclic PLA, with Na^+.

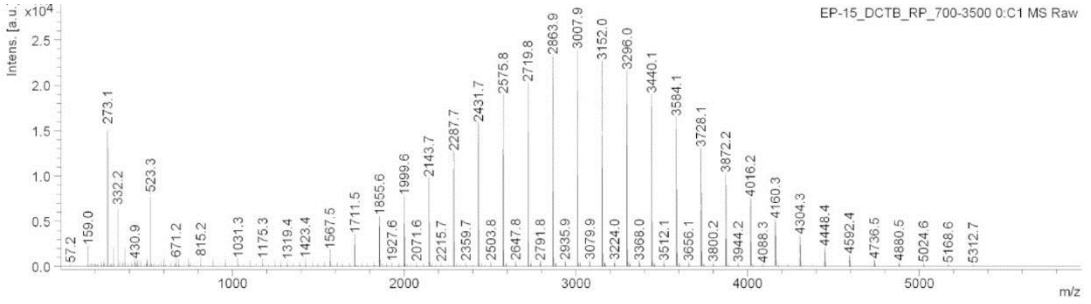

Figure S60. MALDI–TOF spectrum of PLA (2-(4'-Hydroxybenzeneazo)benzoic acid -HABA was used as a matrix) obtained by polymerization of 50 equiv. of *rac*-LA with (*S,S*)-**2** as initiator, in toluene at 40ºC, 24h. The distribution refer to PLA with OH and CH(Me)C(O)OMe end groups, with Na^+.

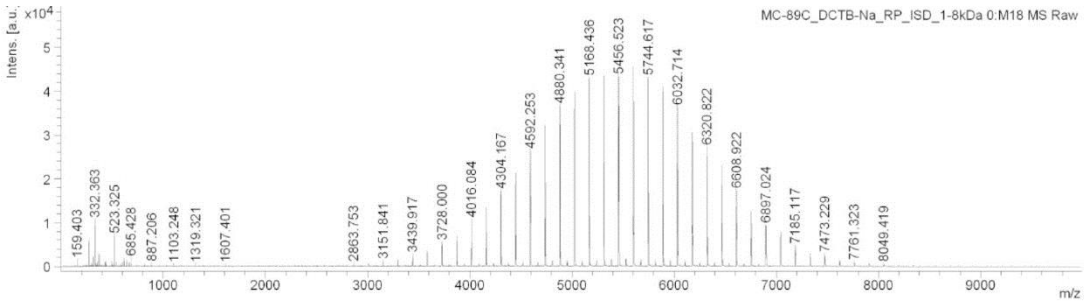

Figure S61. MALDI–TOF spectrum of PLA (T-2-(3-(4-*t*-butyl-phenyl)-2-methyl-2-propenylidene) malononitrile (DCTB) was used as a matrix) obtained by polymerization of 100 equiv. of *rac*-LA with (*S*,*S*)-**2** as initiator, in toluene at r.t., 24h. The distribution refer to PLA with OH and CH(Me)C(O)OMe end groups, with Na^+.

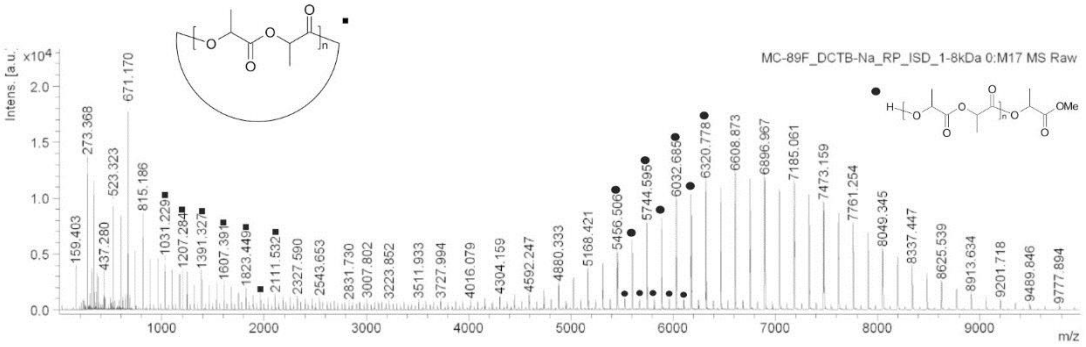

Figure S62. MALDI–TOF spectrum of PLA (T-2-(3-(4-*t*-butyl-phenyl)-2-methyl-2-propenylidene) malononitrile (DCTB) was used as a matrix) obtained by polymerization of 100 equiv. of *rac*-LA with (*S*,*S*)-**2**/ DMEA (1:6) as initiator, in toluene at 40ºC, 24h. The distributions refer to PLA with OH and CH(Me)C(O)OMe end groups and cyclic PLA, with Na^+.

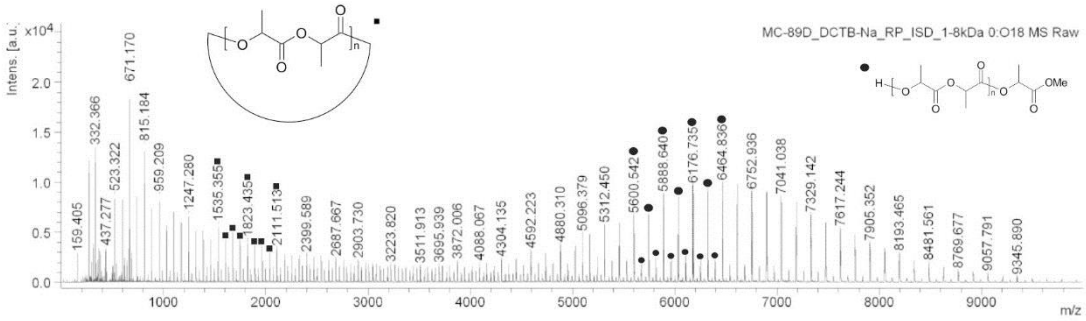

Figure S63. MALDI–TOF spectrum of PLA (T-2-(3-(4-*t*-butyl-phenyl)-2-methyl-2-propenylidene) malononitrile (DCTB) was used as a matrix) obtained by polymerization of 100 equiv. of *rac*-LA with (*S*,*S*)-**2**/pyridine (1:6) as initiator, in toluene at 40ºC, 24h. The distributions refer to PLA with OH and CH(Me)C(O)OMe end groups and cyclic PLA, with Na^+.

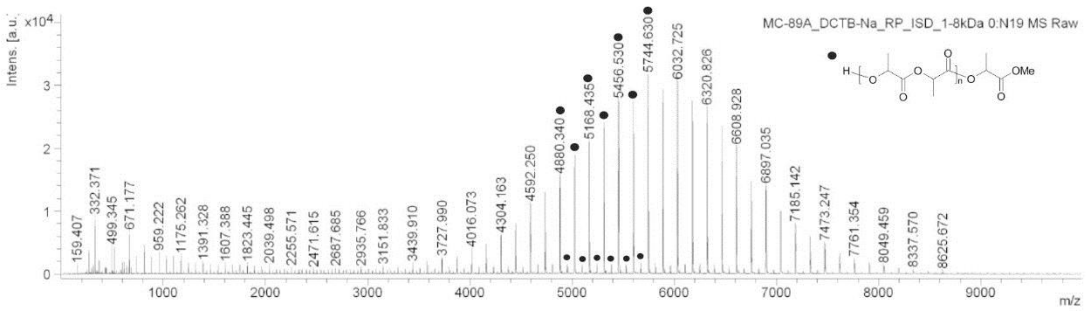

Figure S64. MALDI–TOF spectrum of PLA (T-2-(3-(4-*t*-butyl-phenyl)-2-methyl-2-propenylidene) malononitrile (DCTB) was used as a matrix) obtained by polymerization of 100 equiv. of *rac*-LA with (*S*,*S*)-**2**/pyridine (1:6) as initiator, in toluene at r.t., 24h. The distribution refer to PLA with OH and CH(Me)C(O)OMe end groups, with Na^+ (black dots).

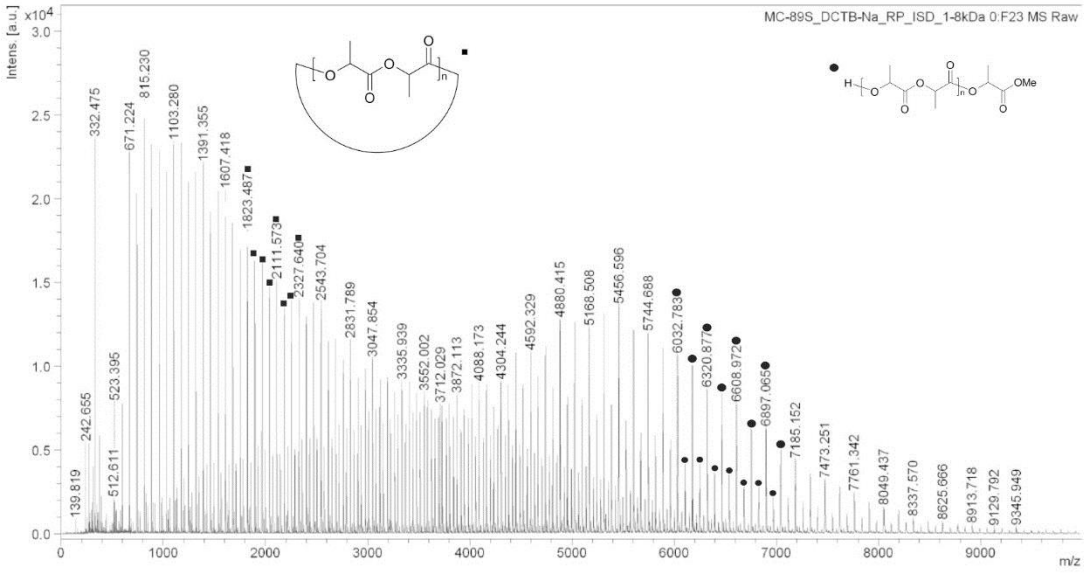

Figure S65. MALDI–TOF spectrum of PLA (T-2-(3-(4-*t*-butyl-phenyl)-2-methyl-2-propenylidene) malononitrile (DCTB) was used as a matrix) obtained by polymerization of 100 equiv. of *rac*-LA with (*S*,*S*)-**2**/γ-picoline (1:6) as initiator, in toluene at 40ºC, 24h. The distributions refer to PLA with OH and CH(Me)C(O)OMe end groups and cyclic PLA, with Na^+.

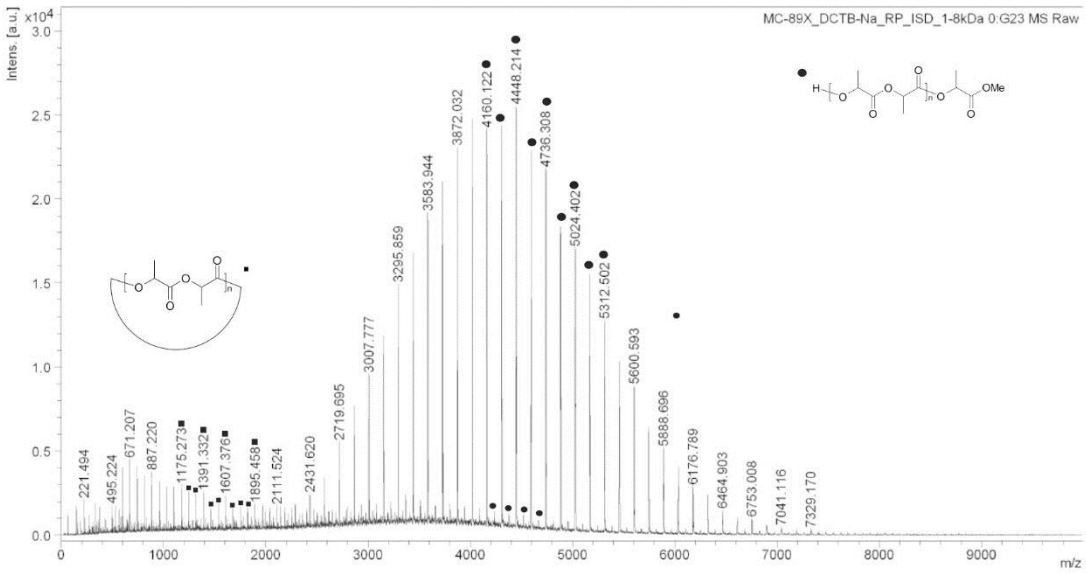

Figure S66. MALDI–TOF spectrum of PLA (T-2-(3-(4-*t*-butyl-phenyl)-2-methyl-2-propenylidene) malononitrile (DCTB) was used as a matrix) obtained by polymerization of 100 equiv. of *rac*-LA with (*S*,*S*)-**2**/γ-picoline (1:6) as initiator, in toluene at r.t., 24h. The distributions refer to PLA with OH and CH(Me)C(O)OMe end groups and cyclic PLA, with Na^+.

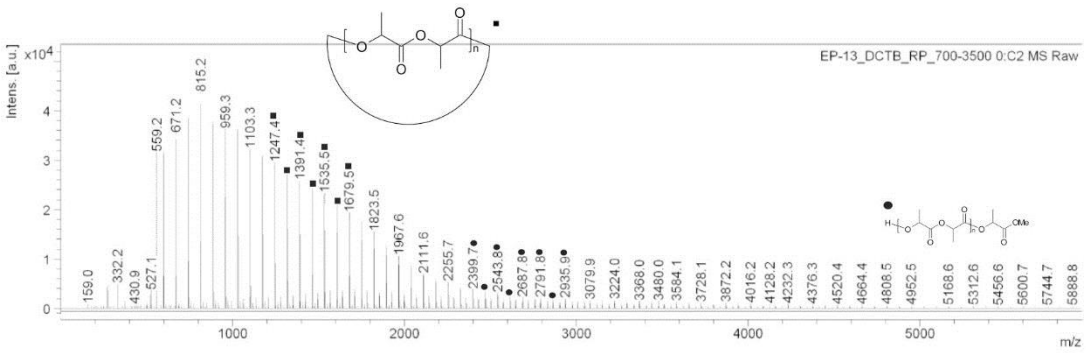

Figure S67. MALDI–TOF spectrum of PLA (T-2-(3-(4-*t*-butyl-phenyl)-2-methyl-2-propenylidene) malononitrile (DCTB) was used as a matrix) obtained by polymerization of 50 equiv. of *rac*-LA with (*S*,*S*)-**2**/DMAP (1:6) as initiator, in toluene at 40ºC, 24h. The distributions refer to PLA with OH and CH(Me)C(O)OMe end groups and cyclic PLA, with Na^+.

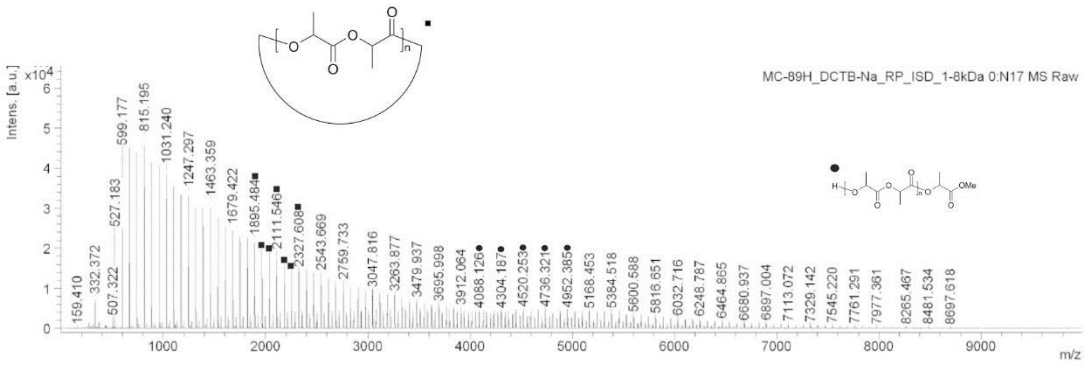

Figure S68. MALDI–TOF spectrum of PLA (T-2-(3-(4-*t*-butyl-phenyl)-2-methyl-2-propenylidene) malononitrile (DCTB) was used as a matrix) obtained by polymerization of 100 equiv. of *rac*-LA with (*S*,*S*)-**2**/DMAP (1:6) as initiator, in toluene at r.t., 24h. The distributions refer to PLA with OH and CH(Me)C(O)OMe end groups and cyclic PLA, with Na^+.

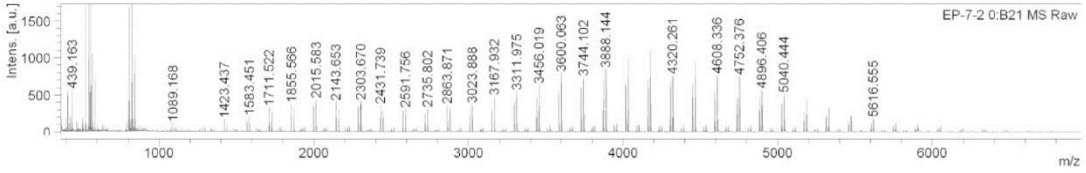

Figure S69. MALDI–TOF spectrum of PLA (T-2-(3-(4-*t*-butyl-phenyl)-2-methyl-2-propenylidene) malononitrile (DCTB) was used as a matrix) obtained by polymerization of 100 equiv. of *rac*-LA with (*S*,*S*)-**2** as initiator, in CH_2Cl_2 at 40ºC, 24h. Two distributions refer to PLA with OH and CH(Me)C(O)OMe end groups, with Na^+ and K^+.

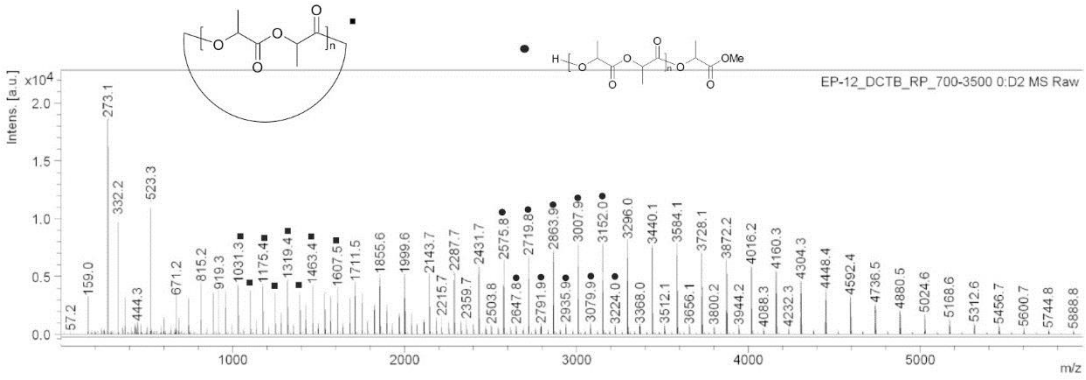

Figure S70. MALDI–TOF spectrum of PLA (T-2-(3-(4-*t*-butyl-phenyl)-2-methyl-2-propenylidene) malononitrile (DCTB) was used as a matrix) obtained by polymerization of 50 equiv. of *rac*-LA with (*S*,*S*)-**2**/pyridine (1:6) as initiator, in CH_2Cl_2 at 40ºC, 24h. The distributions refer to PLA with OH and CH(Me)C(O)OMe end groups and cyclic PLA, with Na^+.

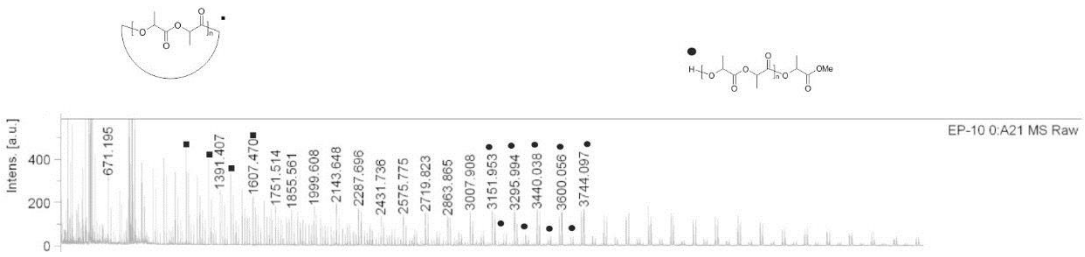

Figure S71. MALDI–TOF spectrum of PLA (2-(4'-Hydroxybenzeneazo)benzoic acid -HABA was used as a matrix) obtained by polymerization of 50 equiv. of *rac*-LA with (*S,S*)-**2**/γ-picoline as initiator, in CH_2Cl_2 at 40ºC, 24h. The distributions refer to PLA with OH and CH(Me)C(O)OMe end groups and cyclic PLA, with Na^+ and K^+.

6) Crystallographic data of (*R,S*)-**1**, (*S,S*)-**2**, (*R,S*)-**2** and **3.**

Table S6 Crystal data and structure refinement details for (*R,S*)-**1**, (*S,S*)-**2**, (*R,S*)-**2** and **3**.

Compound	**(*S,S*)-2**	**(*R,S*)-1**	**3**	**(*R,S*)-2**
Empirical Formula	$C_{12}H_{26}In_2O_6$	$C_{12}H_{26}Ga_2O_6$	$C_{18}H_{28}Ga_2N_2O_2$	$C_{12}H_{26}In_2O_6$
Formula Mass	495.97	405.77	443.86	495.97
Temperature/K	100.0(3)	120.0(1)	120.0(1)	120.0(1)
Crystal system	triclinic	monoclinic	monoclinic	monoclinic
Space Group	*P*1	$P2_1/c$	$P2/n$	$P2_1/c$
a/Å	6.9927(3)	8.15438(13)	8.0739(4)	8.2700(2)
b/Å	8.3025(3)	8.28026(15)	8.5229(5)	8.4677(2)
c/Å	8.4128(3)	12.8297(2)	14.4630(8)	13.1476(3)
α/°	76.086(3)	90	90	90
β/°	83.924(3)	92.0637(14)	97.288(5)	91.014(2)
γ/°	87.628(3)	90	90	90
Volume/Å^3	471.37(3)	865.70(3)	987.20(9)	920.56(4)
Z	1	2	2	2
ρ_{calc}g/cm^3	1.747	1.557	1.493	1.789
μ/mm^{-1}	2.463	3.130	2.741	2.522
F(000)	244.0	416.0	456.0	488.0
Crystal size/mm^3	0.266×0.148×0.014	0.631×0.354×0.116	0.58×0.55×0.32	0.476×0.271×0.258
Reflections collected	20453	40636	8468	14092
Independent Reflections	3846	1870	2362	1885
R_{int}	0.0283	0.0352	0.0237	0.0281
Restraints/Parameters	15/189	0/95	0/112	0/95
Goof on F^2	1.064	1.196	1.157	1.331
Final R_1 ($I > 2\sigma(I)$)	0.0158	0.0188	0.0283	0.0202
Final $wR(F^2)$ ($I > 2\sigma(I)$)	0.0392	0.0459	0.0744	0.0459
Final R_1 (all data)	0.0172	0.0197	0.0309	0.0209
Final $wR(F^2)$ (all data)	0.0398	0.0462	0.0765	0.0461
Largest diff. peak/hole / e Å^{-3}	0.61/−0.54	0.53/−0.29	0.78/−0.77	0.52/−0.41
Flack Parameter	0.01(2)			

[1] Urbańczyk, M.; Bernin, D.; Koźmiński, W.; Kazimierczuk, K. *Analytical Chemistry* **2013**, *85*, 1828−1833.
[2] Chamberlain, B. M.; Cheng, M.; Moore, D. R.; Ovitt, T. M.; Lobkovsky, E. B.; Coates, G. W. *J. Am. Chem. Soc.* **2001**, *123*, 3229−3238
[3] (a) Kasperczyk, J. E. *Macromolecules* **1995**, *28*, 3937–3939. (b) Abbina, S.; Du, G. *ACS Macro Lett.* **2014**, *3*, 689–692.